© 2017. Published by The Company of Biologists Ltd | Development (2017) 144, 2824-2836 doi:10.1242/dev.150680

RESEARCH ARTICLE

Multiple modes of Lrp4 function in modulation of Wnt/β-catenin signaling during tooth development

Youngwook Ahn[1,2,*], Carrie Sims[1], Megan J. Murray[1], Paige K. Kuhlmann[1], Jesús Fuentes-Antrás[1], Scott D. Weatherbee[3] and Robb Krumlauf[1,4,*]

ABSTRACT

During development and homeostasis, precise control of Wnt/β-catenin signaling is in part achieved by secreted and membrane proteins that negatively control activity of the Wnt co-receptors Lrp5 and Lrp6. Lrp4 is related to Lrp5/6 and is implicated in modulation of Wnt/β-catenin signaling, presumably through its ability to bind to the Wise (Sostdc1)/sclerostin (Sost) family of Wnt antagonists. To gain insights into the molecular mechanisms of Lrp4 function in modulating Wnt signaling, we performed an array of genetic analyses in murine tooth development, where Lrp4 and Wise play important roles. We provide genetic evidence that Lrp4 mediates the Wnt inhibitory function of Wise and also modulates Wnt/β-catenin signaling independently of Wise. Chimeric receptor analyses raise the possibility that the Lrp4 extracellular domain interacts with Wnt ligands, as well as the Wnt antagonists. Diverse modes of Lrp4 function are supported by severe tooth phenotypes of mice carrying a human mutation known to abolish Lrp4 binding to Sost. Our data suggest a model whereby Lrp4 modulates Wnt/β-catenin signaling via interaction with Wnt ligands and antagonists in a context-dependent manner.

KEY WORDS: Lrp4, Sostdc1, Mouse, Tooth, Wnt/β-catenin signaling

INTRODUCTION

Wnt/β-catenin signaling plays a pivotal role in the patterning, morphogenesis and growth of a variety of tissues and organs during development and in homeostasis in the adult. Aberrant Wnt signaling activity is causally linked to congenital defects, degenerative diseases and cancers (Clevers and Nusse, 2012). Therefore, understanding the molecular mechanisms that regulate the outputs of this signaling pathway in different *in vivo* contexts and expanding our knowledge of how this is governed through dynamic crosstalk among different tissues and cell types are fundamentally important.

In the Wnt/β-catenin signaling pathway, initiation of signaling requires interaction between Wnt ligands, their frizzled (Fz) receptors and Wnt co-receptors low-density lipoprotein receptor-related proteins 5 and 6 (Lrp5/6) (MacDonald and He, 2012). These interactions on the cell membrane trigger a cascade of intracellular events leading to stabilization and nuclear localization of β-catenin, which together with TCF/LEF transcription factors activates the expression of target genes (MacDonald and He, 2012; MacDonald et al., 2009).

A variety of secreted Wnt antagonists have been shown to inhibit Wnt/β-catenin signaling at the earliest step, presumably by altering or blocking the formation of Wnt/Fz/co-receptor complexes (Cruciat and Niehrs, 2013). *In vitro* binding studies have suggested that, among the Wnt antagonists, sclerostin (Sost) and Wise (also known as Sostdc1) can inhibit Wnt/β-catenin signaling via their ability to bind to the extracellular domains of Lrp5/6 (Ellies and Krumlauf, 2006; Itasaki et al., 2003; Li et al., 2005; Semenov et al., 2005). *Sost* and *Wise* are closely related, as they emerged through genome-wide duplication and divergence, but they display mostly non-overlapping expression patterns (Collette et al., 2013). The function of Sost and Wise in Wnt regulation via direct binding to Lrp5/6 has been further supported by genetic interaction studies in multiples tissues where they play a crucial role in development and homeostasis (Ahn et al., 2010, 2013; Chang et al., 2014b).

Lrp4 has emerged as an important component of the Wnt/β-catenin signaling pathway. The sequence and structure of its extracellular domain are similar to those of Lrp5 and Lrp6. Since the Lrp4 intracellular domain lacks some of the motifs in Lrp5 and Lrp6 known to be essential for Wnt co-receptor function, Lrp4 was proposed to be a negative regulator of Wnt signaling (Herz and Bock, 2002; Johnson et al., 2005; Weatherbee et al., 2006; Willnow et al., 2012). Supporting this idea, overexpression of *Lrp4* results in decreased Wnt/β-catenin signaling activity in cultured cells (Johnson et al., 2005; Li et al., 2010; Ohazama et al., 2008). In *in vitro* binding assays, the extracellular domain of Lrp4 can directly interact with Sost and Wise, suggesting that the Wnt inhibitory function of Lrp4 may depend on its interaction with the Wnt antagonists (Choi et al., 2009; Karner et al., 2010; Ohazama et al., 2008).

In support of interaction between Lrp4 and Wise, mice deficient for *Lrp4* or *Wise* share similar developmental defects in the ectodermal tissues, e.g. teeth, hair and mammary glands (Ahn et al., 2013; Narhi et al., 2012; Ohazama et al., 2008). Early development of these tissues requires reciprocal interactions between the epithelium and underlying mesenchyme, and Wnt signaling along with other major signaling pathways has diverse roles in the control of patterning and morphogenesis at different stages (Ahn, 2015; Balic and Thesleff, 2015; Biggs and Mikkola, 2014). In the tooth germ, *Lrp4* is expressed in the epithelial signaling centers, while *Wise* is expressed in the surrounding epithelial and mesenchymal cells (Ahn et al., 2010; Laurikkala et al., 2003; Ohazama et al., 2008). Mice homozygous for a hypomorphic *Lrp4* allele phenocopy *Wise*-null mice and display various tooth defects, such as supernumerary teeth and molar fusion (Ahn et al., 2010; Ohazama et al., 2008). Since the tooth defects in *Wise*-null mice

[1]Stowers Institute for Medical Research, Kansas City, MO 64110, USA. [2]Department of Molecular Biology, Cell Biology and Biochemistry, Brown University, Providence, RI 02912, USA. [3]Department of Genetics, Yale School of Medicine, New Haven, CT 06520, USA. [4]Department of Anatomy and Cell Biology, University of Kansas Medical Center, Kansas City, KS 66160, USA.

*Authors for correspondence (youngwook_ahn@brown.edu; rek@stowers.org)

Y.A., 0000-0001-5988-7388; M.J.M., 0000-0001-6335-0444; J.F.-A., 0000-0001-5805-2362; S.D.W., 0000-0002-0915-1329

Received 22 February 2017; Accepted 30 June 2017

Development (2017) 144, 2824-2836 doi:10.1242/dev.150680

are caused by elevated Wnt/β-catenin signaling (Ahn et al., 2010), it is possible that Lrp4 functions through its interplay with Wise as part of an important molecular mechanism for modulating Wnt/β-catenin signaling in teeth and other contexts.

To address this question, we utilized gain- and loss-of-function mouse models and *in vitro* reporter assays to investigate how *Lrp4* interacts with *Lrp5/6* and *Wise*. Our genetic interaction analyses focused on tooth development indicate that Lrp4 negatively regulates Wnt/β-catenin signaling to control tooth number, morphology and growth through potentiation of the Wnt inhibitory function of Wise. In addition, our study provides evidence suggesting a Wise-independent role for Lrp4 through its interaction with Wnt ligands and Fz receptors. This work has uncovered novel and diverse mechanisms by which Lrp4 contributes to the modulation of Wnt/β-catenin signaling during development.

RESULTS

Lrp4 deficiency results in survival of R2 vestigial buds and delayed development of the first molar

We investigated the spatiotemporal expression pattern of *Lrp4* in the diastema and molar region of the mandible during early tooth development. In mice, two tooth vestigial buds, namely MS and R2, develop sequentially in the toothless diastema region, but they undergo degeneration without advancing to the cap stage of tooth development (Ahn, 2015; Peterkova et al., 2006) (Fig. 1D). Consistent with a previous report (Ohazama et al., 2008), *Lrp4* transcripts were detected in MS and R2 at E12.5 and E13.5, respectively, similar to the expression pattern of the *TopGal* Wnt activity reporter (Fig. 1A,B). At E14.5, *Lrp4* expression is diminished in degenerating R2, while strong expression is observed in the more proximal region of the dental epithelium where the first molar (M_1) develops (Fig. 1A). Compared with

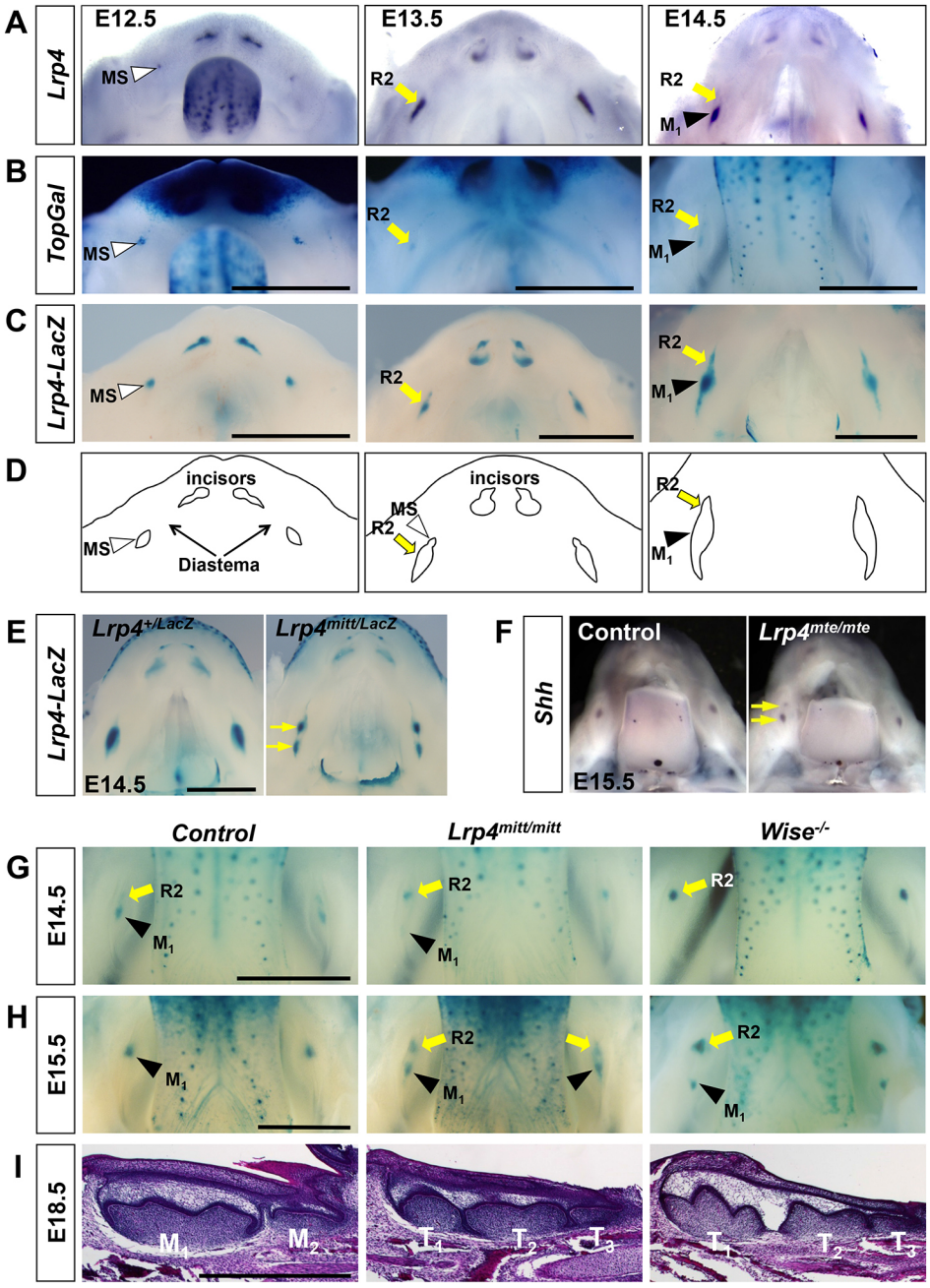

Fig. 1. *Lrp4* deficiency results in survival of the R2 diastema tooth bud in mice. (A) *Lrp4* is expressed in the diastema tooth buds, MS and R2, during normal embryogenesis. Dorsal views of a dissected mandible after *in situ* hybridization for *Lrp4* at three embryonic stages. (B,C) X-Gal-stained mandibles of *TopGal* (B) and $Lrp4^{lacZ}$ (C) mice. (D) Schematic of normal early tooth development in the mandible from A-C. MS and R2 develop in the diastema region, but undergo degeneration. (E,F) X-Gal staining ($Lrp4^{lacZ}$) and *in situ* hybridization (*Shh*) reveal two domains (arrows) of expression indicating survival of R2 in *Lrp4*-null mice. (G-I) Comparison of R2 and M_1 development between *Lrp4*-null and *Wise*-null mice. *TopGal* expression at E14.5 (G) and E15.5 (H) and Hematoxylin and Eosin staining at E18.5 (I) indicate that R2 gives rise to a supernumerary tooth (T_1) in both mutants. However, *Lrp4*-null mice display a shorter distance between R2 and M_1 and a smaller T_1 compared with *Wise*-null mice. Representative images are shown for each genotype ($n \geq 3$). Scale bars: 1 mm.

Development (2017) 144, 2824-2836 doi:10.1242/dev.150680

TopGal, the *Lrp4* expression domain at E13.5 and E14.5 is broader and extends more proximally to reach the proximal end of the tooth germ (Fig. 1A,B). The *Lrp4* expression pattern was further examined in a reporter knock-in model, $Lrp4^{lacZ}$, and found to mimic the *in situ* hybridization pattern of *Lrp4* in the developing incisor and molar regions (Fig. 1A,C). At E14.5, residual β-galactosidase activity marks degenerating R2, which is likely to be due to the stability of the *lacZ* transcript and/or β-galactosidase protein itself. These expression patterns are consistent with roles for *Lrp4* in determining the fate of the diastema buds and M_1.

Supernumerary cheek teeth have been reported with a relatively low frequency in the mandible of mice homozygous for a hypomorphic allele, $Lrp4^{ECD}$ (Ohazama et al., 2008). To clarify whether the supernumerary teeth arise from R2, we analyzed multiple stages of tooth development in mice homozygous for the *Lrp4*-null alleles $Lrp4^{mte}$ or $Lrp4^{mitt}$ (Weatherbee et al., 2006). First, $Lrp4^{mitt}$ mice were crossed with $Lrp4^{lacZ}$ mice and the presence of two domains of reporter expression at E14.5, as compared with controls, suggests that R2 continues to develop in *Lrp4*-null mice (Fig. 1E). Furthermore, an additional *Shh* expression domain is observed distal to M_1 at E15.5, suggesting continuous development of R2 in *Lrp4*-null mice (Fig. 1F). Lastly, narrower and weaker expression domains of enamel knot markers and their downstream target genes indicate abnormal tooth development in *Lrp4*-null mice (Fig. S1).

The progressive development of R2 and M_1 facilitated by loss of *Lrp4* was further monitored utilizing the *TopGal* reporter line and histological sections (Fig. 1G-I). Consistent with the idea of survival of R2 in *Lrp4*-null mice, *TopGal* expression is sustained in R2 at E14.5, whereas M_1 development is delayed as it arises in the more proximal region (Fig. 1G). Survival and continued development of R2 has also been observed in *Wise*-null mice (Ahn et al., 2010). However, there are significant differences in the temporal and spatial expression patterns of *TopGal* in the *Wise* and *Lrp4* mutants (Fig. 1G,H). In *Wise*-null mice, the continued development of R2 is greatly enhanced, as evidenced by a strong and enlarged *TopGal* expression domain at E14.5. Conversely, M_1 development is greatly delayed in *Wise*-null mice, as the *TopGal* expression domain marking M_1 is not detected until E15.5. R2 continues to develop to form a prominent supernumerary tooth, T_1 at E18.5 (Fig. 1I). By contrast, in *Lrp4*-null mice R2 is maintained with a relatively modest level of *TopGal* expression at E14.5-15.5 and the delay in M_1 development in *Lrp4*-null mice is not as significant as in *Wise*-null mice (Fig. 1G,H). The distance between R2 and M_1 is variable and generally shorter in *Lrp4*-null mice than in *Wise*-null mice at E15.5. Consistent with these differences, T_1, which originates from R2, is smaller in *Lrp4*-null mice at E18.5 (Fig. 1I). Together with reduced expression of the enamel knot markers and their targets, this suggests that R2 is not undergoing accelerated development in *Lrp4*-null mice and this is associated with a weak inhibition of M_1.

Lrp4 deficiency ameliorates *Wise*-null tooth defects

The comparative analyses above highlight differences as well as similarities in tooth phenotypes of *Lrp4* or *Wise* mutant mice, suggesting the possibility of overlapping and independent mechanisms by which Lrp4 and Wise control tooth development. With respect to overlapping mechanisms, it is possible that similar effects of deficiency of *Lrp4* or *Wise* on tooth development arise through their involvement in the regulation of a common signaling pathway. Our primary focus was the Wnt/β-catenin signaling pathway, as mutants of these two genes show altered Wnt signaling activity (Fig. 1G). We performed genetic interaction studies in order to explore this possibility and gain a deeper mechanistic understanding of their roles in tooth germs. We first investigated how Lrp4 and Wise impact each other's function during tooth development by crossing $Lrp4^{mitt}$ mice with *Wise*-null mice and monitoring *TopGal* expression patterns in double mutants. This enabled us to determine whether inactivation of both genes results in significant changes in Wnt signaling and tooth defects compared with the individual mutants (Fig. 2A,B). $Lrp4^{mitt/mitt};Wise^{-/-}$ mice display no sign of exacerbated tooth defects and instead show variable distance between R2 and M_1, similar to $Lrp4^{mitt/mitt}$ mice. This indicates that tooth defects of $Lrp4^{mitt/mitt};Wise^{-/-}$ mice are milder than those of *Wise*-null mice, in which a greater distance between R2 and M_1 is invariably maintained.

Since $Lrp4^{mitt/mitt}$ mice die immediately after birth (Weatherbee et al., 2006), we also used $Lrp4^{ECD/ECD}$ mice to evaluate how these changes during embryogenesis are translated into the number, size and shape of adult teeth. We observed that embryonic tooth development is similarly disrupted in $Lrp4^{ECD/ECD}$ mice as in *Lrp4*-null mice (Fig. S2). After obtaining $Lrp4^{ECD};Wise$ compound mutants, we categorized mandibular and maxillary tooth patterns into distinct groups based on the severity of fusion and presence of the supernumerary cheek teeth (T_1) to aid our comparative analyses of these tooth phenotypes (Fig. 2C, Fig. S3). In the mandible, $Lrp4^{ECD/ECD}$ mice display tooth defects similar to, but generally milder than, those of *Wise*-null mice (Fig. 2C). In contrast to the full penetrance of the T_1 phenotype in *Wise*-null mice, only 32% of $Lrp4^{ECD/ECD};Wise^{+/-}$ mice display T_1. This indicates that in the *Lrp4*-deficient mice, even though R2 initially escapes degeneration, the majority of R2 buds fail to develop into T_1 and instead merge into M_1 during later development. In addition to T_1, *Wise*-null mice frequently develop lateral supernumerary teeth and fusions between neighboring cheek teeth due to overgrowth, and these defects are rarely observed in $Lrp4^{ECD/ECD}$ or $Lrp4^{ECD/ECD};Wise^{+/-}$ mice (Fig. 2C; data not shown). In the maxilla, both mutants display fusions of distal molars, with a higher penetrance observed in *Wise*-null mice (Fig. S3).

Comparison of mandibular tooth phenotypes among $Lrp4^{ECD};Wise$ compound mutants indicated that $Lrp4^{+/+};Wise^{-/-}$ mice display the most severe defects. Removing one allele of *Lrp4* in a $Wise^{-/-}$ background ($Lrp4^{+/ECD};Wise^{-/-}$) and then the second *Lrp4* allele ($Lrp4^{ECD/ECD};Wise^{-/-}$) progressively reduces the severity of the phenotypes (Fig. 2C). For example, fully or partially separated T_1 was observed with 100%, 66% and 46% penetrance in $Lrp4^{+/+};Wise^{-/-}$, $Lrp4^{ECD/ECD};Wise^{-/-}$ and $Lrp4^{ECD/ECD};Wise^{+/-}$ mice, respectively. A similar trend was observed in the maxilla of the compound mutants (Fig. S3). In order to rule out the possibility that the released extracellular domain of Lrp4 expressed from the $Lrp4^{ECD}$ allele (Dietrich et al., 2010) has an effect on tooth development and complicates our analyses, we performed the same analyses with another hypomorphic mutant, $Lrp4^{mdig}$, combined with $Lrp4^{mitt}$ mice and obtained similar results (Fig. S4). These genetic analyses indicate that Lrp4 makes an independent contribution to the generation of the severe tooth defects in *Wise*-null mice.

Reduced dosages of *Lrp5* and *Lrp6* rescue the tooth defects of *Lrp4* mutant mice

The more mild phenotypes observed upon loss of *Lrp4* in *Wise* mutants suggests that Lrp4 might exert a stimulatory effect on Wnt/β-catenin signaling in a Wise-independent manner during tooth

Development (2017) 144, 2824-2836 doi:10.1242/dev.150680

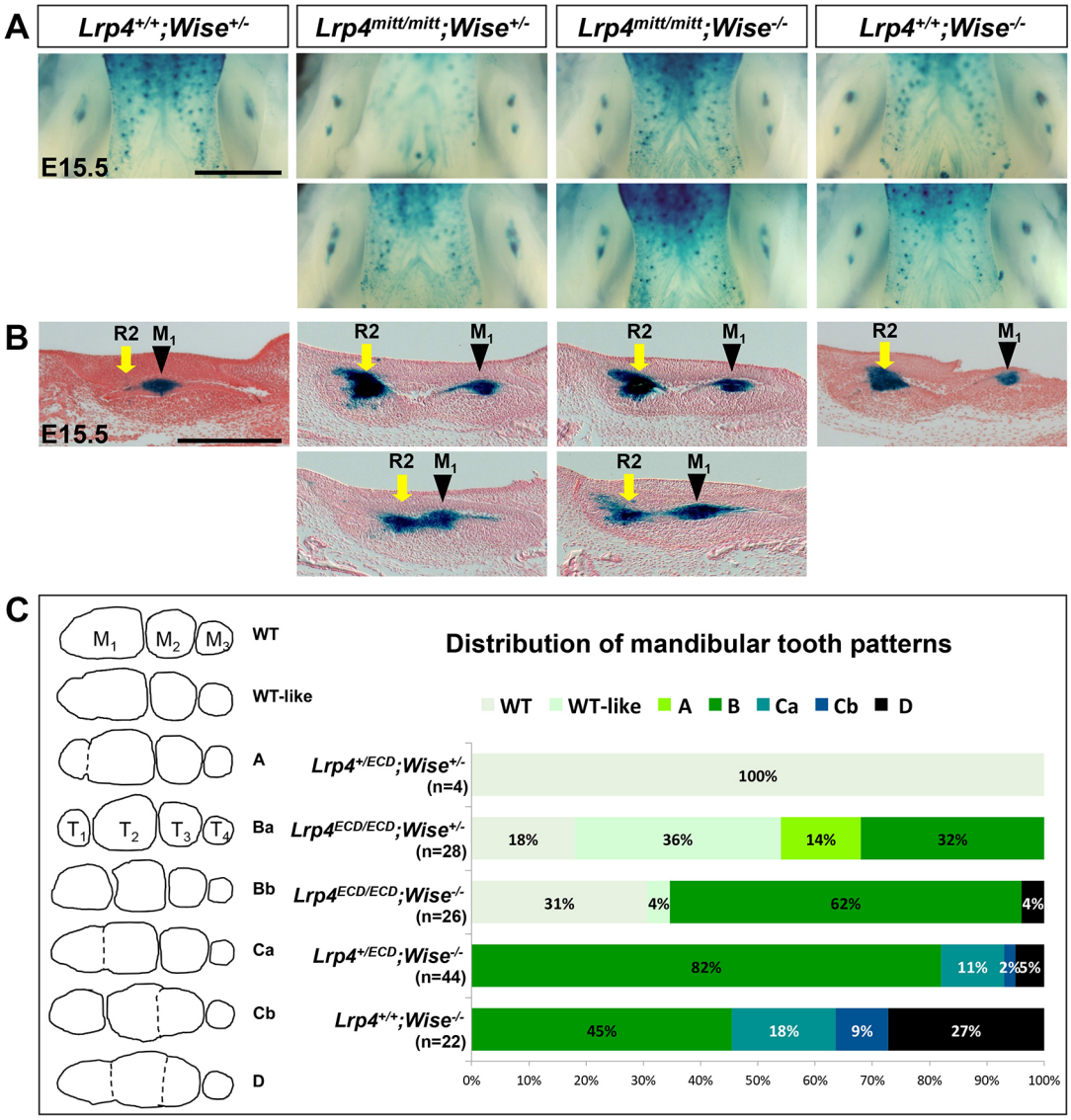

Fig. 2. *Lrp4* deficiency ameliorates *Wise*-null molar defects. (A,B) *Lrp4*$^{mitt/mitt}$;*Wise*$^{-/-}$ mice display variable, but generally shorter, distance between R2 and M_1, mimicking *Lrp4*$^{mitt/mitt}$ mice. Whole-mount images (A) and histological sections (B) of *TopGal* stained E15.5 mandibles are shown. Scale bars: 1 mm in A; 0.5 mm in B. (C) *Lrp4* deficiency ameliorates tooth defects of *Wise*-null mice in a dosage-dependent manner. Mandibular tooth patterns are categorized based on the number, size and fusion of cheek teeth (left). Distribution of different tooth patterns among littermates of the *Lrp4*^{ECD} and *Wise*-null combinatorial mutants (right).

development. To explore whether elevated Wnt/β-catenin signaling is causally associated with the tooth defects in *Lrp4* mutants, we crossed *Lrp4*^{ECD} mice with *Lrp5*- and *Lrp6*-null mice and examined the effect of reduced *Lrp5/6* gene dosages on the tooth phenotypes among littermates. A supernumerary incisor is observed with ~85% penetrance in the maxilla of *Lrp4*$^{ECD/ECD}$ and this phenotype is rescued by reduced dosages of *Lrp5/6* (Fig. 3A). In the mandible, a supernumerary cheek tooth (T_1) is observed with high frequency among *Lrp4*$^{ECD/ECD}$ mice (90%, *n*=26) in this strain background, and reduced dosages of *Lrp5/6* lead to a lower frequency of T_1 (Fig. 3B, top). In the maxilla, molar fusions common in *Lrp4*$^{ECD/ECD}$ mice are rescued by reduced dosages of *Lrp5/6* (Fig. 3B, bottom). This dosage-dependent rescue of *Lrp4* tooth defects by deficiency in *Lrp5/6* implies that elevated Wnt/β-catenin signaling is primarily responsible for the abnormalities in incisor and molar development in *Lrp4* mutant mice. Similar to the results from our previous study with *Wise*-null mice (Ahn et al., 2010), we observed differences between *Lrp5* and *Lrp6* in their ability to rescue different aspects of the tooth defects with reduced gene dosages.

Although genetic analyses in teeth (Fig. 3A,B) and other tissues (Ahn et al., 2013) indicate that Lrp4 and Lrp5/6 generally have opposite roles in Wnt signaling, our data lead us to hypothesize that this relationship might be altered in the absence of Wise, revealing a potential Wise-independent role for Lrp4 in positively modulating Wnt/β-catenin signaling. To genetically test this idea, we investigated how the *Lrp4*-null allele *Lrp4*^{mitt} interacts with *Lrp5* and *Lrp6* in *Wise*-null mice. Interestingly, inactivating a copy of *Lrp4* enhances the effect of reduced *Lrp5* and *Lrp6* gene dosage on *Wise*-null tooth defects and results in further rescue in the mandible (Fig. 3C). These data suggest that, in the absence of Wise, Lrp4 can positively regulate Wnt/β-catenin signaling, mimicking the normal roles of Lrp5/6. Together, these genetic analyses have uncovered dual roles for Lrp4. In the presence of Wise, Lrp4 negatively regulates Wnt/β-catenin signaling as its major mechanism of action

Development (2017) 144, 2824-2836 doi:10.1242/dev.150680

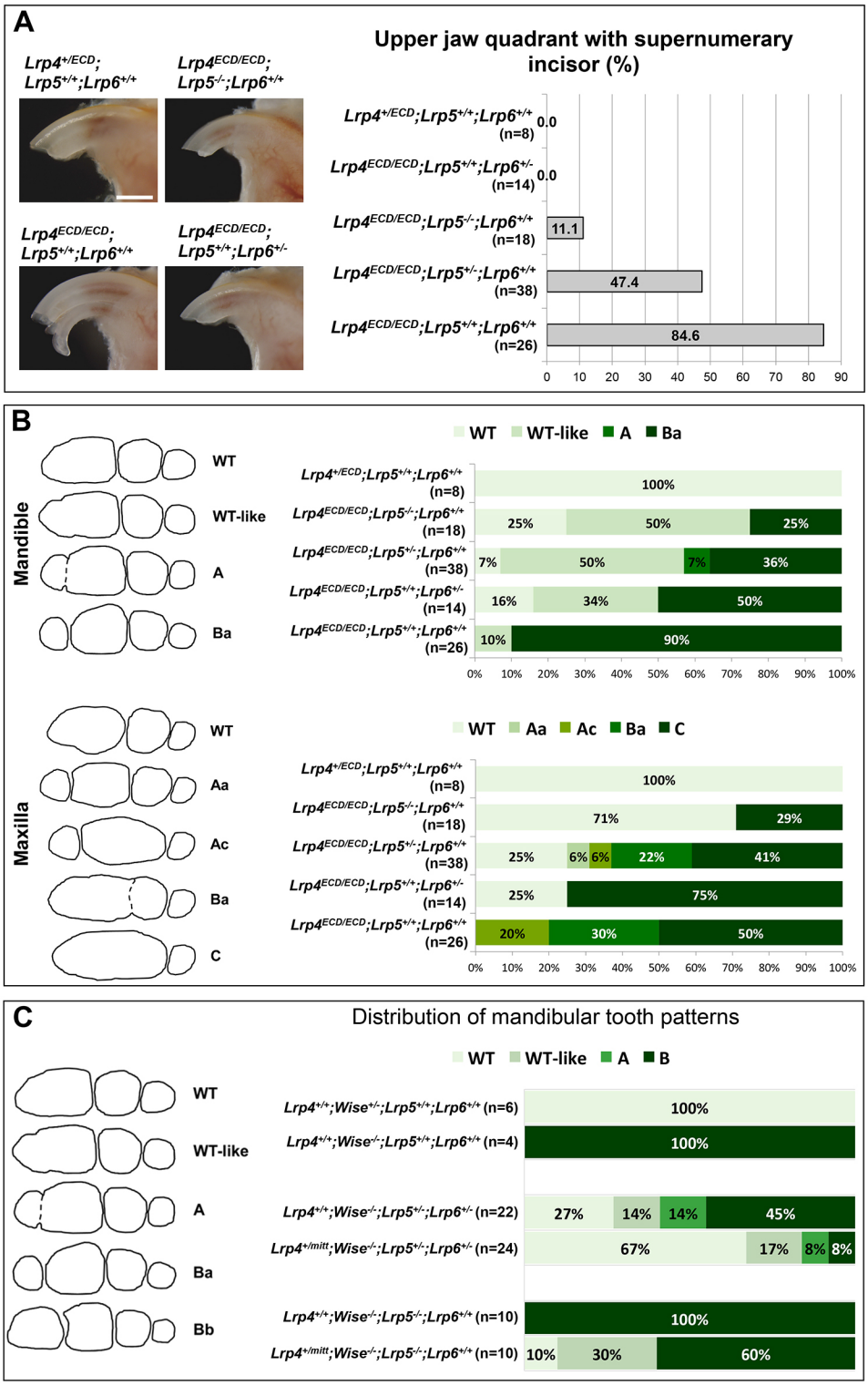

Fig. 3. Genetic interaction of *Lrp4* with *Lrp5* and *Lrp6* in tooth development. (A) Reduced dosages of *Lrp5* and *Lrp6* rescue the supernumerary incisor phenotype of $Lrp4^{ECD/ECD}$ mice. Scale bar: 1 mm. (B) Reduced dosages of *Lrp5* and *Lrp6* ameliorate molar abnormalities of $Lrp4^{ECD/ECD}$ mice. (C) Reduced dosages of *Lrp4*, *Lrp5* and *Lrp6* ameliorate *Wise*-null tooth defects in an additive manner.

to control tooth number and growth. In the absence of Wise, Lrp4 can play a stimulatory role in Wnt/β-catenin signaling through a different mechanism. This illustrates that Wise can alter the impact of Lrp4 on Wnt signaling in a context-dependent manner.

Lrp4 is necessary for *Wise* to inhibit tooth development

Overexpression of *Wise* in the dental epithelium leads to delay and hypoplasia in molar development (Ahn et al., 2010). We investigated whether this *Wise* gain-of-function phenotype requires *Lrp4*. Since *K14-Wise* mice were not able to breed, we instead utilized the Tet-off system, in which the keratin 14 (*K14*) promoter drives expression of a transactivator (tTA) in the first transgene (*K14-tTA*), and in the absence of doxycycline tTA in turn activates the expression of *Wise* and *eGFP* in the second transgene (*tetO-Wise*) (Ahn et al., 2013) (Fig. 4A). In *K14-tTA;tetO-Wise* mice, eGFP, which serves as an indicator of *Wise* expression, is detected specifically in the dental epithelium (Fig. 4B). After birth, molars appear to be smaller and the third maxillary molar is

Development (2017) 144, 2824-2836 doi:10.1242/dev.150680

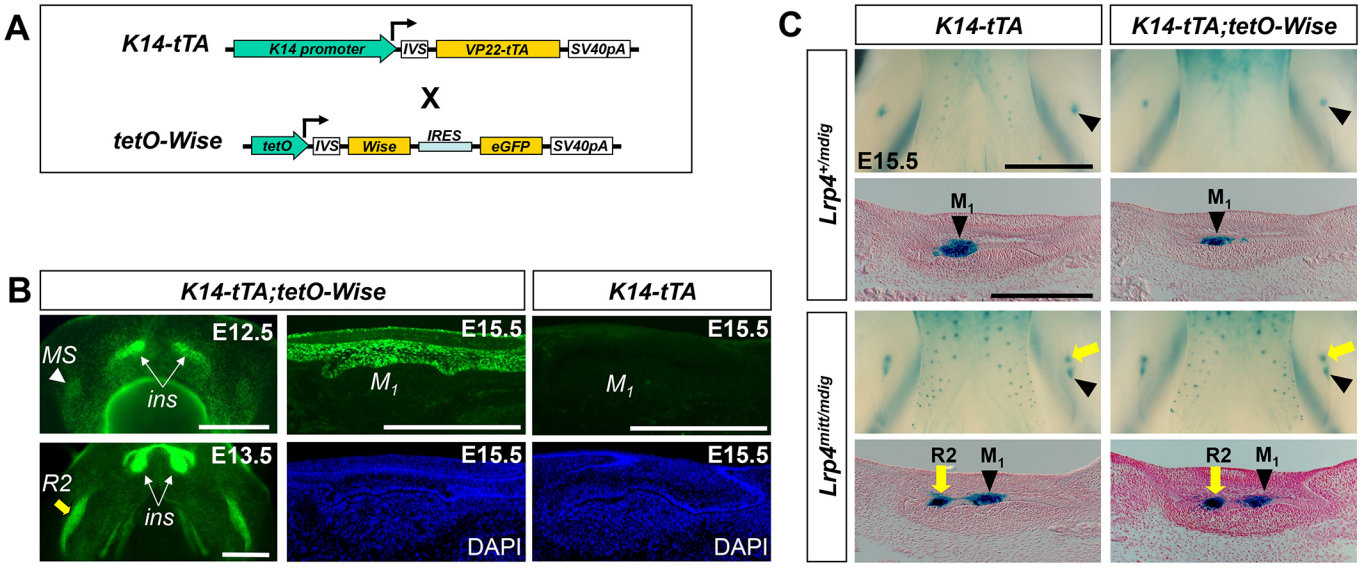

Fig. 4. *Lrp4* is necessary for *Wise* to inhibit tooth development. (A) The Tet-off binary transgenic system that overexpresses *Wise* in the dental epithelium. (B) In *K14-tTA;tetO-Wise* mice, eGFP fluorescence is seen in the incisor (ins) and the MS and R2 buds, as shown in dorsal views of the dissected mandible (left). A frozen section of M_1 from *K14-tTA;tetO-Wise* mice (top, middle) indicates that eGFP is restricted to the epithelial cells at E15.5, whereas no eGFP is detectable in the control (top, right). Scale bars: 0.5 mm. (C) *Lrp4* is required for the *Wise* gain-of-function tooth phenotypes. Normally, *Wise* overexpression suppresses tooth development (*Lrp4*$^{+/mdig}$, compare right with left). In *Lrp4*-deficient mice, *Wise* overexpression has no significant effect on tooth development (*Lrp4*$^{mitt/mdig}$, compare right with left). Scale bars: 1 mm (whole mount) and 0.5 mm (section).

frequently missing, reminiscent of the phenotypes of the *K14-Wise* mice (Fig. S5).

These two transgenic lines were then crossed with *Lrp4* mutant lines to generate *Lrp4*-deficient mice overexpressing *Wise*. In *Lrp4*$^{+/mdig}$ mice, overexpression of *Wise* results in a reduced domain of the dental epithelial cells expressing *TopGal* and in hypoplasia of tooth germs at E15.5 (Fig. 4C). In *Lrp4*$^{mitt/mdig}$ mice, R2 continues to develop, similar to our observation in other *Lrp4* mutants, and this phenotype is not altered by overexpression of *Wise* (Fig. 4C). The lack of a *Wise* gain-of-function phenotype in *Lrp4*-deficient tooth germs suggests that Wise depends on Lrp4 to exert its Wnt inhibitory activity in tooth development.

Ectopically expressed *Lrp4* disrupts tooth development in a *Wise* dosage-dependent manner

With its highly restricted expression pattern in the dental epithelium, *Lrp4* might provide a spatial cue for the action of Wise, which is broadly expressed in the tooth germ (Ahn et al., 2010; Laurikkala et al., 2003; Ohazama et al., 2008). To test this idea, we performed gain-of-function analyses of *Lrp4* by generating a *tetO-Lrp4* expression line (Fig. 5A). The transgenic line was first tested for its ability to rescue the limb defects of *Lrp4* mutants. For this rescue experiment, we also generated *Lrp4BAC-tTA* driver lines, which express *tTA* in the *Lrp4* expression domains, including the apical ectodermal ridge (AER) of limb buds (Fig. S6A). Severe patterning defects in the distal limb of *Lrp4* mutants are fully rescued in *Lrp4BAC-tTA;tetO-Lrp4* mice, indicating that functional Lrp4 protein is expressed from the transgene (Fig. S6B).

The *tetO-Lrp4* line was then crossed with the *K14-tTA* line to test the effect of ectopic *Lrp4* expression in the dental epithelium (Fig. 5B). Intriguingly, in *K14-tTA;tetO-Lrp4* mice, overexpression of *Lrp4* results in temporary survival of R2 (Fig. 5G,H), which fails to form a supernumerary tooth and instead merges into M_1 at later stages, leading to abnormal cusp patterning in the distal region of M_1 (Fig. 5C,D). We hypothesized that ectopic expression of *Lrp4* disrupts the normal distribution and/or function of Wise and hence causes elevation in Wnt/β-catenin signaling in the epithelial signaling center of R2. This idea was supported by the observation that a half dose of *Wise* exacerbates the *Lrp4* gain-of-function tooth phenotypes. *Wise*$^{+/-}$*;K14-tTA;tetO-Lrp4* mice display more sustained survival of R2 (Fig. 5I,J), which gives rise to a supernumerary cheek tooth in the mandible (Fig. 5E,F). In the maxilla, overgrowth/fusion of distal molars was frequently observed in *Wise*$^{+/-}$*;K14-tTA;tetO-Lrp4* mice reminiscent of *Wise*-null tooth phenotypes (Fig. 5C′-J′). The idea was also tested by simultaneously overexpressing *Wise* and *Lrp4* in the dental epithelium. Tooth development is further delayed in *K14-tTA;tetO-Wise;tetO-Lrp4* compared with *K14-tTA;tetO-Wise* mice, as evidenced by much smaller domains of *TopGal* expression at E15.5-E16.5 (Fig. 5K-R). Together, these data support a model whereby Lrp4 directs Wise function in the epithelial signaling center of developing teeth via direct interactions.

Lrp4-Lrp6 fusions uncover domain-specific roles for Lrp4

To gain insights into the molecular interactions between Lrp4, Wise and Lrp5/6 uncovered from our *in vivo* studies, we utilized an *in vitro* reporter system in which the activity of Wnt/β-catenin signaling is measured in a human cell line expressing different combinations of the proteins (Fig. S7). As expected, expression of Wnt1 or human WNT3A leads to a dramatic increase in Wnt reporter activity, indicating that the amount of Wnt ligand is a limiting factor for signaling activation in the cultured cells. Lrp4 and Wise antagonize the activity of WNT3A as well as Wnt1, consistent with the Wnt inhibitory potential of Lrp4 and Wise over these two classes of Wnt ligands. Co-expression of *Lrp4* and *Wise* leads to further reduction in Wnt reporter activity.

The extracellular domain (ECD) of Lrp4 is similar to those of Lrp5 and Lrp6, whereas its intracellular domain (ICD) is distinct. To investigate whether this difference in the ICD underlies the Wnt inhibitory role of Lrp4, we generated chimeric proteins of Lrp4 and

Development (2017) 144, 2824-2836 doi:10.1242/dev.150680

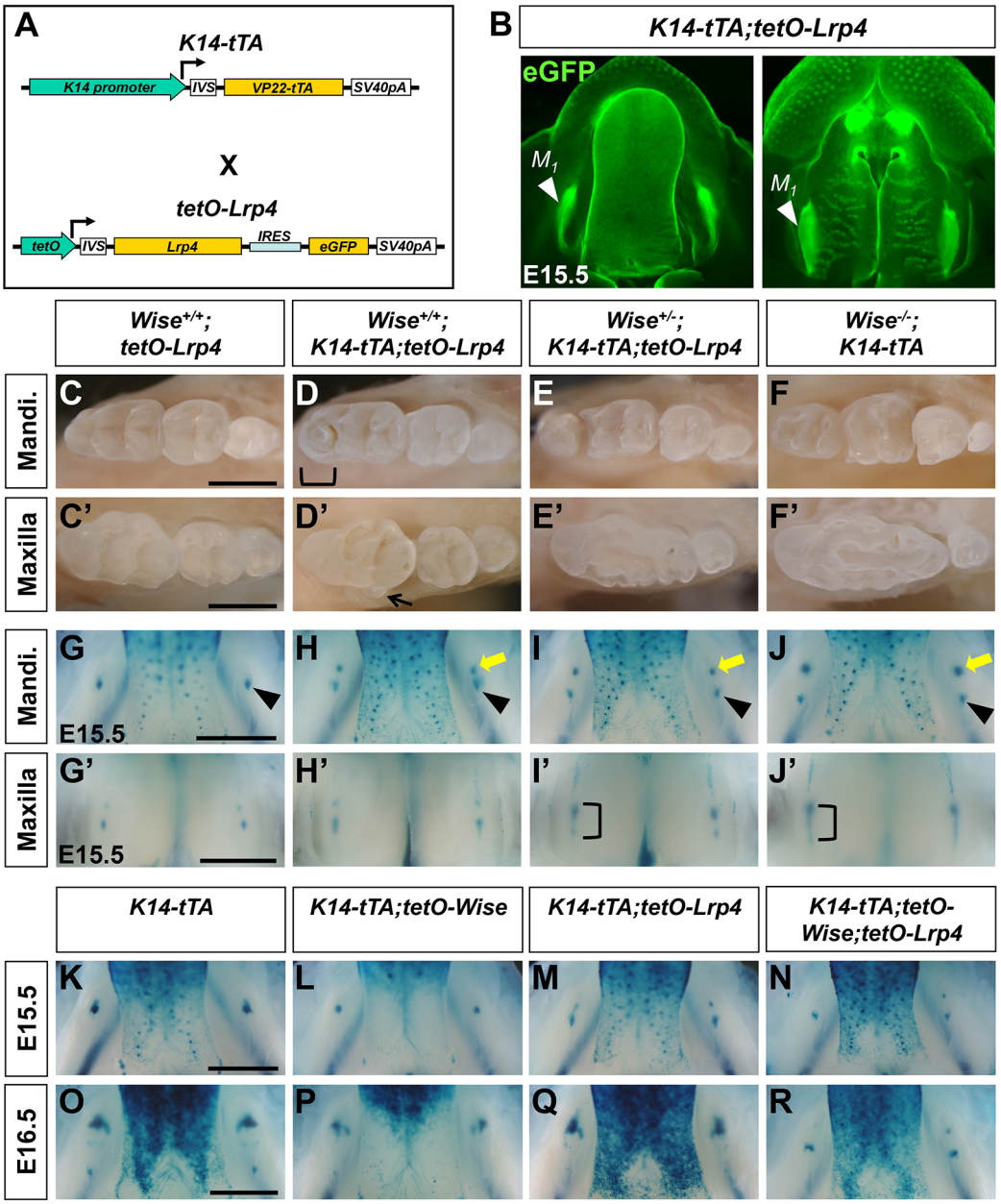

Fig. 5. *Lrp4* overexpression disrupts tooth development in a *Wise*-dependent manner. (A) The Tet-off binary transgenic system that overexpresses *Lrp4* in the dental epithelium. (B) eGFP fluorescence is seen in M_1 of the mandible (left) and maxilla (right) in *K14-tTA;tetO-Lrp4* mice. (C-F′) *Lrp4* overexpression in otherwise wild-type mice results in abnormal cusp patterns in the distal part of the mandibular M_1 (D, bracket) and a lateral supernumerary tooth in the maxilla (D′, arrow). In *Wise*$^{+/-}$ mice, *Lrp4* overexpression results in a supernumerary cheek tooth in the mandible (E) and fusion of distal teeth in the maxilla (E′). (G-J′) X-Gal-stained mandibles (G-J) and maxilla (G′-J′) with *TopGal*. In the mandible, *Lrp4* overexpression results in survival of R2 (yellow arrow), which is close to M_1 (arrowhead) (H). In *Wise*$^{+/-}$*;K14-tTA;tetO-Lrp4* mice, R2 maintains distance from M_1 after survival in the mandible (I), and the diastema bud and M_1 are often fused in the maxilla (I′) as in *Wise*-null mice (J′, bracket). (K-R) X-Gal-stained mandibles with *TopGal* at E15.5 indicate that simultaneous overexpression of *Wise* and *Lrp4* strongly inhibits tooth development (K-N). At E16.5, *TopGal* expression domains remain much smaller in mice overexpressing both *Wise* and *Lrp4* as compared with mice overexpressing *Wise* only (O-R). Scale bars: 1 mm.

Lrp6 and tested their activity in the cultured cells (Fig. 6A-C). In general, the level of the Wnt co-receptor appeared to be another limiting factor, as co-expression of Lrp6 with the Wnt ligands results in further elevation of reporter activity. When Wnt ligands and Lrp6 are co-expressed, Wise is ineffective in suppressing the reporter activity. Lrp4ECD-Lrp6ICD (L4L6) mimics Lrp6, facilitating activation of Wnt/β-catenin signaling by Wnt1 or WNT3A, although not as efficiently as Lrp6 itself. Conversely, Lrp6ECD-Lrp4ICD (L6L4) mimics Lrp4, leading to a reduction in Wnt reporter activity. These results suggest that the respective ICD determines whether these two Lrp receptors play a stimulatory or inhibitory role in Wnt/β-catenin signaling. Furthermore, the Wnt stimulatory activity of L4L6 implies that Lrp4ECD can act like Lrp6ECD and interact with the Wnt ligands. L4L6 is more responsive to Wise co-expression, resulting in a more dramatic decrease in reporter activity compared with Lrp6. By contrast, L6L4 alone is more potent than Lrp4 in Wnt inhibition and this inhibitory activity is not enhanced by Wise co-expression. This

Development (2017) 144, 2824-2836 doi:10.1242/dev.150680

suggests that Wise interacts with Lrp4ECD more efficiently than with Lrp6ECD to impact receptor activity.

Gain- and loss-of-function *in vivo* studies support domain-specific roles for Lrp4

We tested the *in vivo* relevance of the above chimeric receptor findings by expressing *Lrp6* and L4L6 in transgenic mice utilizing the Tet-off system. As predicted, expression of *Lrp6* in the dental epithelium results in the ectopic formation of tooth bud-like structures accompanied by *TopGal* expression, indicating increased activation of Wnt/β-catenin signaling (Fig. 6D). A similar phenotype was observed when L4L6 is expressed in the dental epithelium, consistent with its *in vitro* activity of stimulating Wnt signaling (Fig. 6D). Together, our *in vitro* and *in vivo* data indicate that the ECDs of Lrp4 and Lrp6 share an ability to interact with both Wnt ligands and Wise.

It has been shown that the ICD is dispensable for Lrp4 function in the neuromuscular junction as a receptor for agrin (Choi et al., 2013; Gomez and Burden, 2011). In this regard, it is unclear whether the tooth defects of $Lrp4^{ECD/ECD}$ mice result from lack of anchorage to the cell membrane or from lack of ICD. Therefore, we utilized CRISPR/Cas9 technology to generate a new *Lrp4* allele, $Lrp4^{\Delta ICD}$, which produces an Lrp4 protein lacking the ICD. Mice homozygous for this allele are viable and display tooth defects comparable to those of $Lrp4^{ECD/ECD}$ mice, indicating that the ICD is essential for the normal function of Lrp4 in tooth development (Fig. 6E). The majority (77.8%, n=36) of $Lrp4^{\Delta ICD/\Delta ICD}$ mice show a typical pattern of T_1, T_2-T_3 and T_4, with rare occurrence of later supernumerary teeth (6.7%) in the mandible. Some (16.7%) show signs of incomplete separation of T_1 and T_2 teeth, resulting in the pattern T_1-T_2-T_3 and T_4. Overall, the tooth defects of $Lrp4^{\Delta ICD/\Delta ICD}$ mice are milder than those of *Wise*-null mice based on criteria such as the relative size of T_1 and the frequency of lateral supernumerary teeth. This highlights the important role of the Lrp4 ICD in tooth development.

$Lrp4^{R1170W}$ mutation mimics *Wise*-null tooth phenotypes

The relatively mild tooth phenotypes of various *Lrp4* mutants and the genetic interaction of *Lrp4* with *Wise* and *Lrp5/6* together suggest the existence of Wise-independent roles for Lrp4 in tooth development. Validation of this hypothesis requires a context in which the Wise-dependent roles are blocked while other aspects of Lrp4 function are preserved. Since no such mouse models were available, we created mice carrying the human R1170W mutation (G to T), which has been shown to abolish SOST binding to LRP4 (Leupin et al., 2011). This is likely to abolish Wise binding to Lrp4, without affecting the normal cell membrane localization of Lrp4 (Leupin et al., 2011). Mice homozygous for the $Lrp4^{R1170W}$ allele are viable, indicating that the Lrp4 function in the neuromuscular junction is not significantly affected. To our surprise, $Lrp4^{R1170W/R1170W}$ mice display tooth phenotypes more severe than those of $Lrp4^{ECD/ECD}$ and $Lrp4^{\Delta ICD/\Delta ICD}$ mice and comparable to those of *Wise*-null mice (Fig. 7A). For example, T_1 is typically longer with multiple cusps and lateral supernumerary teeth are frequently observed in $Lrp4^{R1170W/R1170W}$ mice. This suggests that the single amino acid substitution is sufficient to prevent Lrp4 from inhibiting Wnt/β-catenin signaling during tooth development. It also implies that the substitution efficiently blocks the Lrp4-Wise interaction.

Severe syndactyly and/or oligodactyly are common to all known *Lrp4* mutant models and are attributed to disruption in AER

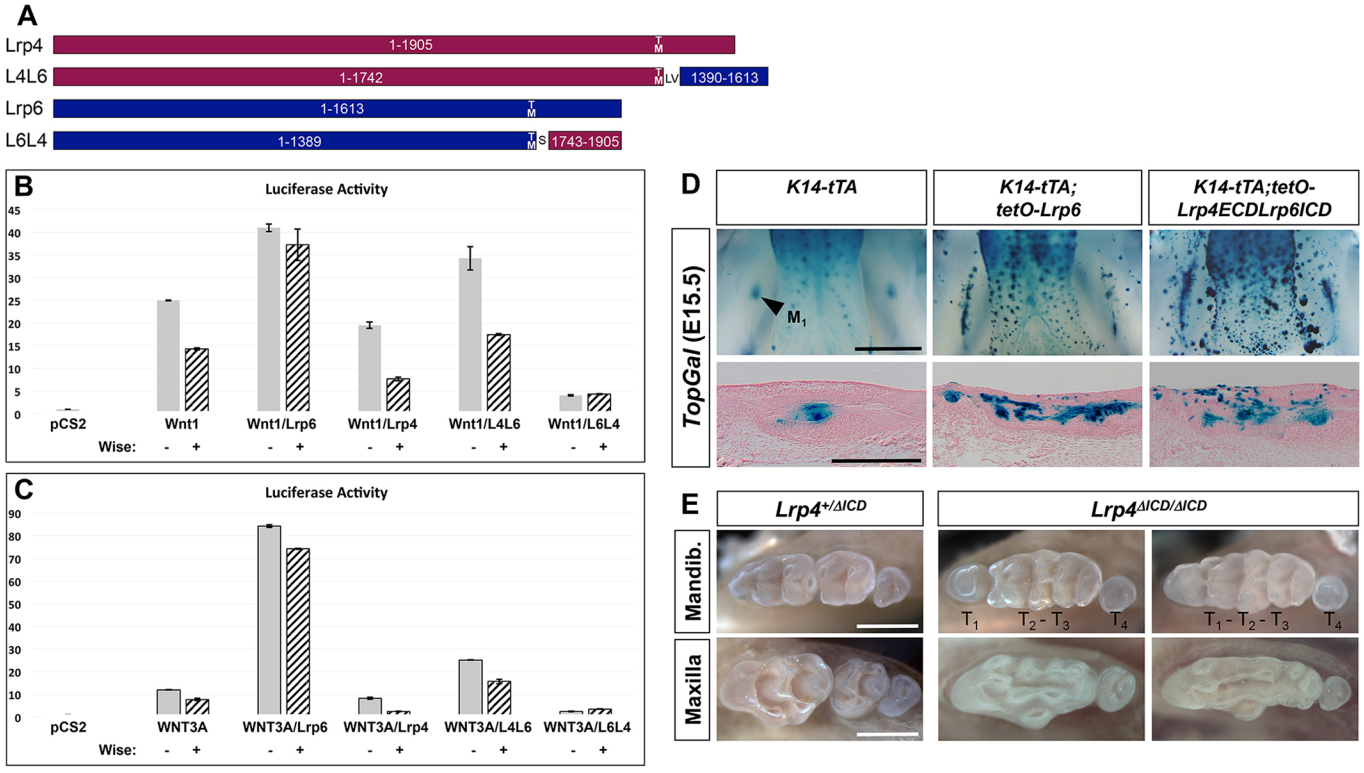

Fig. 6. Domain-specific roles for Lrp4. (A) Lrp4-Lrp6 fusion proteins. Numbers within the boxes indicate amino acid residues (Lrp4, NP_766256.3; Lrp6, NP_032540.2) encoded by each construct. TM, transmembrane domain. LV and S are linker peptides. (B,C) Relative luciferase activity from *TOPflash* reporter after transfecting HEK 293T cells with constructs driving expression of *Wnt1* (B) or *WNT3A* (C) in combination with other proteins. An empty vector (pCS2) was used to show the basal level of reporter activity. (D) Overexpression of *Lrp6* and *Lrp4ECD-Lrp6ICD* results in forced activation of Wnt/β-catenin signaling in the dental epithelium. (E) Removal of the intracellular domain of Lrp4 results in abnormal tooth development. Scale bars: 1 mm (whole mount) and 0.5 mm (section).

Development (2017) 144, 2824-2836 doi:10.1242/dev.150680

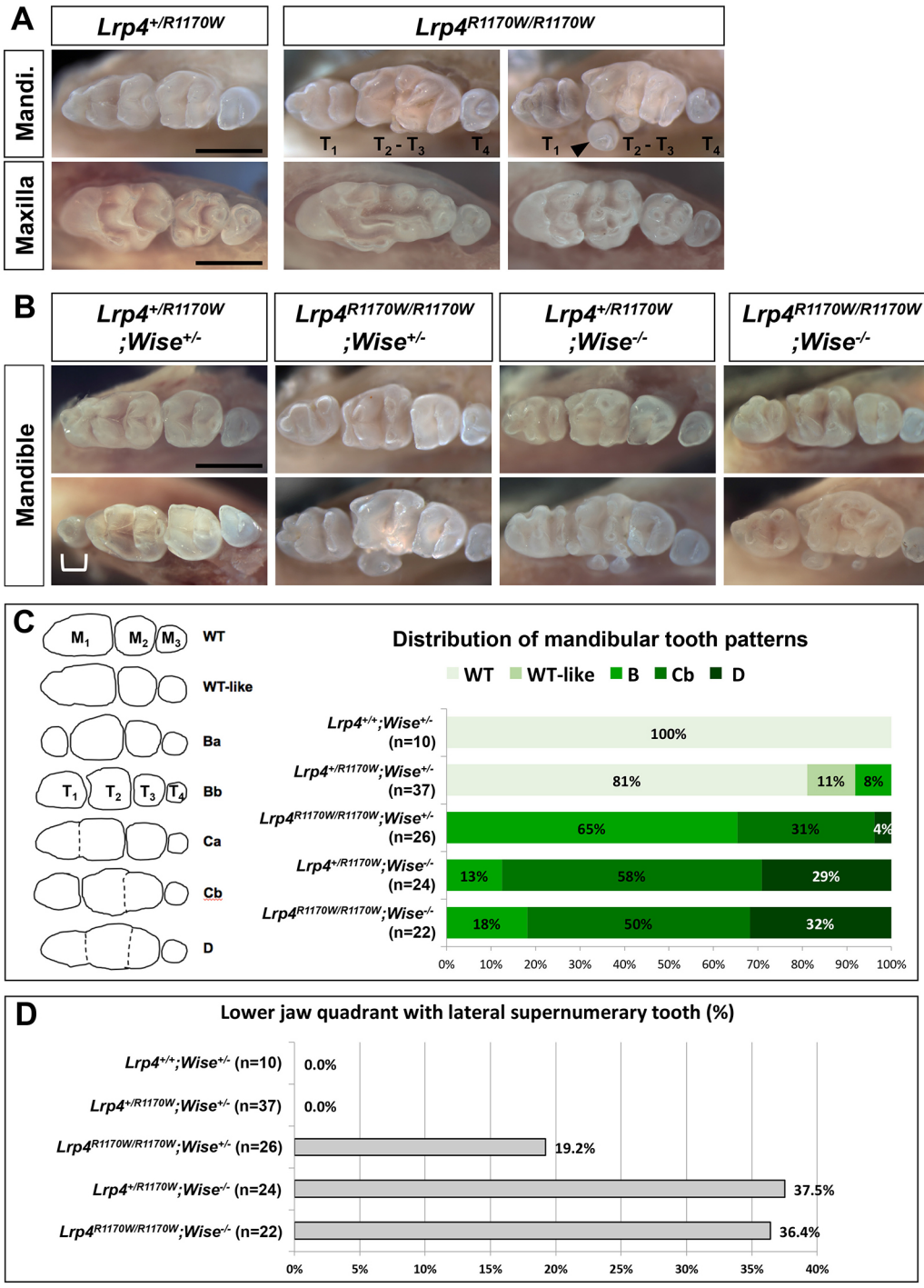

Fig. 7. Tooth defects of mice with the R1170W mutation. (A) *Lrp4*$^{R1170W/R1170W}$ mice display strong tooth defects such as a larger T_1 and lateral supernumerary teeth (arrowhead). (B) Genetic interaction between the *Lrp4*^{R1170W} and *Wise*-null alleles. Some transheterozygotes develop a supernumerary tooth (bracket) distal to M_1. Two representative samples are shown for each genotype. Scale bars: 1 mm. (C,D) Distribution of mandibular tooth patterns (C) and penetrance of the lateral supernumerary tooth phenotype (D) among mice carrying the *Lrp4*^{R1170W} and *Wise*-null alleles.

patterning (Li et al., 2010; Pohlkamp et al., 2015; Simon-Chazottes et al., 2006; Weatherbee et al., 2006). Similarly, *Lrp4*$^{\Delta ICD/\Delta ICD}$ mice display severe defects in distal limbs (Fig. S8). Surprisingly, *Lrp4*$^{R1170W/R1170W}$ mice display no apparent limb defects, indicating that the arginine residue is not essential for the Lrp4 function in patterning of the AER (Fig. S8). Since the limb defects are causally associated with elevated Wnt/β-catenin signaling (Ahn et al., 2013), our data suggest that Lrp4 negatively regulates Wnt/β-catenin signaling largely independently of Wise/Sost during early limb patterning. Supporting this idea, single and double mutants for *Wise* and *Sost* display no, or very subtle, limb defects (Collette et al., 2013).

Lrp4^{R1170W} mice were then crossed with *Wise*-null mice to test whether the *Lrp4*^{R1170W} allele interacts with the *Wise*-null allele differently, as compared with other *Lrp4* alleles. Whereas no tooth defects are present in *Lrp4*$^{+/R1170W}$ and *Wise*$^{+/-}$ mice, a small portion

Development (2017) 144, 2824-2836 doi:10.1242/dev.150680

(8.1%, n=37) of transheterozygotes display T_1, which has presumably developed from R2 (Fig. 7B,C). In contrast to *Lrp4*$^{ECD/ECD}$;*Wise*$^{-/-}$ and *Lrp4*$^{mitt/mdig}$;*Wise*$^{-/-}$ mice, in which the *Wise*-null tooth phenotypes are ameliorated, there is no significant difference in the severity of tooth defects between *Lrp4*$^{+/R1170W}$;*Wise*$^{-/-}$ and *Lrp4*$^{R1170W/R1170W}$;*Wise*$^{-/-}$ mice (Fig. 7B-D). Together, these genetic data support a model whereby Lrp4 mediates the Wnt inhibitory function of Wise in tooth development, and the R1170 residue is essential for the Lrp4-Wise interaction. Since *Lrp4*$^{R1170W/R1170W}$ mice phenocopy *Wise*-null mice with severe tooth defects, we conclude that Lrp4 has a Wise-independent Wnt stimulatory activity that is not disrupted by the missense mutation.

DISCUSSION

In this study, an extensive series of genetic analyses in teeth provide strong experimental evidence for a hypothesis that Lrp4 and Wise physically interact with each other to negatively regulate Wnt/β-catenin signaling. The findings also provide new insights into molecular mechanisms associated with interactions between Lrp4, Wise and the Wnt co-receptors Lrp5/6. We demonstrate that Lrp4 acts as both inhibitor and activator of the Wnt/β-catenin pathway dependent upon its interactions with Wise. *In vitro* and *in vivo* chimeric receptor analyses unveil roles played by the extracellular and intracellular domains of Lrp4 in its interplay with Wnt ligands, antagonists and Lrp5/6 co-receptors. By generating a mouse model of a human missense mutation, we demonstrate that Wise-dependent and Wise-independent roles for Lrp4 can be separated. These findings broaden our understanding of mechanisms that incorporate different inputs to achieve precise spatiotemporal control of signaling activity during development.

Similarities and differences in tooth defects of *Lrp4*-deficient and *Wise*-deficient mice

In this study, we uncovered not only similarities, but also significant qualitative and quantitative differences in tooth phenotypes between *Wise*-deficient and *Lrp4*-deficient mice. We utilized a *Wise*-null allele and a series of *Lrp4*-null and hypomorphic alleles and carefully analyzed tooth phenotypes to rule out the possibility that these differences result from partial inactivation of the gene or differences in strain backgrounds. In mice deficient for either of the genes, the diastema bud R2 escapes from degeneration and gives rise to a supernumerary cheek tooth distal to M_1 in the mandible. Whereas this phenotype is ∼100% penetrant in *Wise*-null mice regardless of strain background, *Lrp4* mutants display a wide-range of penetrance (30-90%) in different strain backgrounds. One possible explanation for this difference is that the degree of alteration in signaling activity caused by *Lrp4* deficiency is relatively low so that penetrance of the phenotype is affected by genetic modifiers. We discovered that, unlike in *Wise*-null mice, R2 fails to maintain distance from M_1 and often becomes merged into M_1 in *Lrp4*-null mice. In the lateral inhibition model, an existing tooth delays development of the next tooth (Kavanagh et al., 2007). This suggests that a lack of accelerated development of R2, and hence reduced lateral inhibition on M_1, results in relatively early development of M_1 in *Lrp4* mutants. As R2 loses its inhibitory advantage over M_1, it is more likely to be merged into M_1, mimicking the outcome in normal tooth development. We also discovered that other aspects of tooth defects are milder in *Lrp4* mutants. For example, lateral supernumerary teeth are rarely observed and overgrowth is not common in the mandible of *Lrp4* mutants compared with *Wise*-null mice.

We observed that molar defects are more severe in the maxilla than in the mandible in both *Wise*-deficient and *Lrp4*-deficient mice leading to overgrowth and fusion of the distal teeth, consistent with published observations (Ahn et al., 2010; Ohazama et al., 2008). This less variable fusion phenotype is attributed to elevation of Wnt/β-catenin signaling to a much higher level in the maxilla of the mutants, as significant rescue of the defect requires removal of at least two copies of *Lrp5* and *Lrp6* (Ahn et al., 2010) (this study).

Wise-dependent and Wise-independent roles for Lrp4 in tooth development

That there are significant differences in the severity of tooth defects caused by deficiency of *Lrp4* or *Wise* is in line with the two proteins also having independent roles. In this regard, our previous study in embryonic mammary gland development revealed stage-specific roles for Lrp4 and Wise (Ahn et al., 2013). The earlier and more severe patterning defects in *Lrp4* mutant mice compared with *Wise*-null mice may be attributed to a Wise-independent role for Lrp4 in the mammary placodes. Unexpectedly, in *Lrp4;Wise* double-homozygous mutants the tooth defects are ameliorated compared with those of *Wise*-null mice. Furthermore, removing a copy of *Lrp4* on top of reduced dosages of *Lrp5/6* results in further rescue of *Wise*-null tooth phenotypes. Since both *Lrp4* and *Wise* single mutants display tooth defects associated with elevated Wnt signaling and these defects are rescued by reduced dosages of *Lrp5/6*, inhibition of Wnt/β-catenin signaling is likely to be the major mechanism of action of Lrp4 in tooth development. However, our data point to the presence of an additional Wnt stimulatory role for Lrp4 that is independent of Wise. In this scenario, the net effect of *Lrp4* deficiency would still be an increase in Wnt/β-catenin signaling, as the inhibitory activity of Lrp4 in the presence of Wise is greater than its stimulatory activity. Consequently, overall tooth phenotypes of *Lrp4* mutants would be milder than those of *Wise*-null mice, in which Lrp4 maintains its stimulatory activity. Lack of the stimulatory activity would explain the amelioration of *Wise*-null phenotypes in *Lrp4*$^{ECD/ECD}$;*Wise*$^{-/-}$ and *Lrp4*$^{mitt/mdig}$;*Wise*$^{-/-}$ mice. It is possible that this stimulatory activity is enhanced in the absence of Wise, contributing to the severe tooth defects of *Wise*-null mice.

Our gain-of-function analyses provided further insights into the interplay between *Wise* and *Lrp4* in tooth development. Whereas overexpression of *Wise* in the dental epithelium suppresses tooth development, excess *Wise* fails to exert any significant effect on the dynamics of R2 and M_1 development in *Lrp4*-deficient mice. This dependence of Wise on Lrp4 suggests that Lrp4 is required for most, if not all, aspects of Wise function in the inhibition of Wnt/β-catenin signaling. *Lrp4* gain-of-function tooth phenotypes are more intriguing as they mimic, to a certain degree, *Lrp4* loss-of-function phenotypes. Since *Lrp4* expression is temporally dynamic and spatially restricted, it is likely that ectopic overexpression disrupts *Lrp4* function in its normal expression domain, which overlaps with the epithelial signaling centers. It is possible that this represents the Wise-independent Wnt stimulatory activity of Lrp4 mentioned above. We speculated that secreted Wise proteins become a limiting factor when Lrp4 is in excess, which can alter the distribution and function of Wise. This idea was supported by the observation that a reduced dosage of Wise exacerbates *Lrp4* gain-of-function phenotypes and that simultaneous overexpression of *Wise* and *Lrp4* results in stronger suppression of tooth development.

Dissecting domain-specific roles for Lrp4

Our chimeric receptor analyses indicate that the ICD determines whether Lrp4 and Lrp5/6 play a stimulatory or inhibitory role in

Development (2017) 144, 2824-2836 doi:10.1242/dev.150680

Wnt/β-catenin signaling. The observation that the ECDs of Lrp4 and Lrp6 are somewhat interchangeable suggests that the ECDs of Lrp4 and Lrp5/6 can interact with a similar set of signaling molecules, such as Wnt ligands and antagonists. This might be linked to Wise-independent roles for Lrp4 in certain contexts. Interestingly, Lrp4ECD appeared to be more responsive to co-expression of Wise, and Lrp6ECD more responsive to co-expression of Wnt ligands. This difference might reflect a higher affinity of Lrp4 to Wise and a lower affinity to Wnt ligands.

Our analyses of $Lrp4^{\Delta ICD/\Delta ICD}$ mice indicate that the ICD is essential for Lrp4 function in limb and tooth development, but dispensable in the neuromuscular junction. Since the mutant mice display tooth defects comparable to those observed in mice with other *Lrp4* mutations that presumably disrupt most aspects of Lrp4 function, it is likely that removal of the ICD leads to loss of both Wise-dependent and -independent functions of Lrp4. Anchorage to the cell membrane alone appears insufficient for Lrp4 function in the modulation of Wnt/β-catenin signaling. It remains to be investigated whether the ICD is required for proper trafficking to the cell membrane or is directly involved in the modulation of Wnt/β-catenin signaling.

In postnatal bone, loss of *Lrp4* in osteoblasts leads to increased bone mass reminiscent of bone phenotypes observed in mice deficient for *Sost* (Chang et al., 2014a; Collette et al., 2012; Li et al., 2008; Xiong et al., 2015). Human patients with the *LRP4* mutation R1170W display bone overgrowth and the mutation results in reduced binding to SOST and abolishes the LRP4 function as a facilitator of SOST in cultured cells (Leupin et al., 2011). The severe tooth phenotypes of $Lrp4^{R1170W}$ mice and the lack of amelioration of *Wise*-null tooth defects in $Lrp4^{R1170W/R1170W};Wise^{-/-}$ mice together suggest that Wise and Sost bind to the same domain of Lrp4 to inhibit Wnt/β-catenin signaling. *Sost* and *Wise* originate from a common ancestral gene (Collette et al., 2013), but have since diverged from each other. This study provides evidence that despite significant differences (less than 40% amino acid identity) between the two antagonists, Wise interacts similarly with Lrp4 to regulate Wnt/β-catenin signaling during tooth development. $Lrp4^{R1170W}$ mice provide a valuable *in vivo* model in which the antagonist-dependent Wnt inhibitory role of Lrp4 is abolished while its antagonist-independent roles in the modulation of Wnt and other signaling pathways are retained.

Multiple modes of Lrp4 function in the modulation of Wnt/β-catenin signaling

With a large ECD possessing multiple protein-protein interaction motifs, Lrp4 can potentially interact with an array of signaling molecules to control Wnt/β-catenin signaling. Based on findings from the current and earlier studies, we propose a model involving multiple modes of action deployed by Lrp4 to modulate Wnt/β-catenin signaling (Fig. 8).

Modes I and II describe two mechanisms for Wise-dependent Wnt inhibitory activity of Lrp4. Lrp4 might act as an anchor/presenter molecule for Wise. During tooth development, Lrp4 recruits Wise to the epithelial signaling centers to inhibit Wnt/β-catenin signaling. Wise might be presented to Lrp5/6 via Lrp4, resulting in displacement of Wnt ligands and inhibition of signaling (mode I, Fig. 8A). Alternatively, Lrp4 together with Wise might compete with Lrp5/6 for binding to Fz receptors (mode II, Fig. 8B).

In some developmental contexts, Lrp4 might inhibit Wnt/β-catenin signaling independently of Wise. In this scenario, Lrp4 might compete with Lrp5/6, interfering with the formation of Wnt/Fz/co-receptor complexes (mode III, Fig. 8C).

The current study also discovered a Wise-independent Wnt stimulatory role for Lrp4. It remains to be investigated whether this role involves a direct interaction between Lrp4 and Wnt/β-catenin

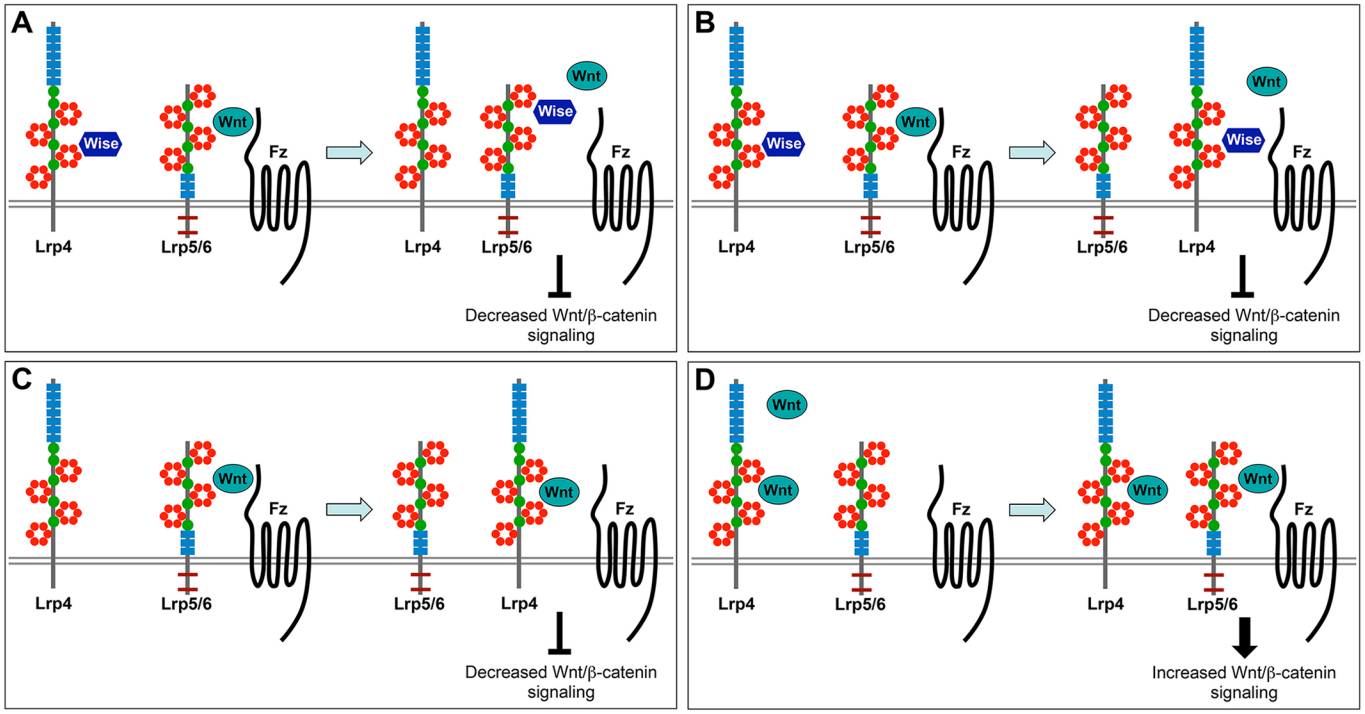

Fig. 8. Proposed modes of Lrp4 function in different contexts. (A) Mode I: Lrp4 presents Wise to Lrp5/6 resulting in displacement of Wnt ligands and inhibition of Wnt/β-catenin signaling. (B) Mode II: Lrp4 in the presence of Wise competes with Lrp5/6 for binding to Fz receptors. (C) Mode III: in the absence of Wise, Lrp4 inhibits Wnt/β-catenin signaling by competing with Lrp5/6 for Wnt ligands and/or Fz receptors. (D) Mode IV: in the absence of Wise, Lrp4 binds to Wnt ligands and presents them to Lrp5/6 for activation of Wnt/β-catenin signaling.

Development (2017) 144, 2824-2836 doi:10.1242/dev.150680

signaling or is mediated via another signaling pathway. Lrp4 might bind to Wnt ligands and present them to Lrp5/6 for activation of Wnt/β-catenin signaling (mode IV, Fig. 8D). This mode might be advantageous when the signaling needs to be activated rapidly in a defined domain and then turned off by expression of the antagonists.

Our findings suggest that Lrp4 acts as a modulator of Wnt/β-catenin signaling, integrating multiple inputs, and that its mode of action is determined by the presence and relative concentration of signaling molecules such as Wnt ligands, antagonists and receptors. Although it is unknown how Lrp4 regulates different signaling pathways, our study demonstrates that different domains of Lrp4 can be linked to pathway-specific roles, opening a door to more effective and safer therapeutics to treat disease conditions caused by abnormal LRP4 function (Shen et al., 2015).

MATERIALS AND METHODS

Mouse strains

TopGal, *Lrp4*^{mitt}, *Lrp4*^{mte}, *Lrp4*^{mdig}, *Lrp4*^{ECD}, *Wise*-null, *Lrp5*-null, *Lrp6*-null, *K14-tTA* and *tetO-Wise* mice were described previously (Ahn et al., 2013; DasGupta and Fuchs, 1999; Johnson et al., 2005; Kato et al., 2002; Pinson et al., 2000; Simon-Chazottes et al., 2006; Weatherbee et al., 2006) (Table S1). All experiments involving mice were performed under approved protocols issued to R.K. as the principal investigator by the Institutional Animal Care and Use Committee of the Stowers Institute for Medical Research (Protocol ID: 2016-0164).

Generation of *Lrp4BAC-tTA*, *tetO-Lrp4*, *tetO-Lrp6* and *tetO-Lrp4ECD-Lrp6ICD* transgenic mice

The *Lrp4BAC-tTA* was constructed by inserting *VP22-tTA-SV40pA* (Gossen and Bujard, 1992) in-frame into the first coding exon of *Lrp4* in a 134 kb *Lrp4* BAC clone (Ahn et al., 2013) using bacterial recombination technology (Lee et al., 2001). The *tetO* constructs were generated by replacing the *Wise* ORF in the *tetO-Wise* construct (Ahn et al., 2010) with coding sequences of *Lrp4*, *Lrp6* and *Lrp4ECD-Lrp6ICD*. Transgenic founders were generated by pronuclear injection of linearized constructs into (C57BL/10JxCBA)F2 embryos. F0 founder or N1 mice carrying individual *tetO* transgenes were crossed with *K14-tTA* mice to identify expression lines that drive *eGFP* expression in the presence of tTA.

Generation of *Lrp4*^{lacZ}, *Lrp4*$^{\Delta ICD}$ and *Lrp4*^{R1170W} mice using CRISPR/Cas9 technology

Gene editing was achieved by pronuclear injection of *pX330* plasmids expressing *Cas9* and single guide RNA (sgRNA) (Cong et al., 2013; Mashiko et al., 2013; Wang et al., 2013). Twenty base pair seed sequences preceding the PAM sequence (NGG) at the target loci were cloned into the *pX330 Bbs*I site. *Lrp4*^{lacZ} mice carrying an in-frame insertion of *lacZ* into the first exon were generated in (C57BL/10JxCBA)F2 embryos by co-injecting a donor plasmid (15 ng/µl) and *pX330* plasmid (3 ng/µl) with 5′-GGCGCCCTGCTCTGCGCACA-3′ as a seed sequence (supplementary Materials and Methods).

Lrp4$^{\Delta ICD}$ mice were generated by introducing two stop codons after Lys1751 using an oligo donor (5′-ATACCTATAAAGTTCTCAACTGA-TTTCAGCCCGATTTTTCCTCTTGAAGACACAGAAAATGATAACA-GACGGATCCTGGAATGGGAAACCTGACCTATAGCAACCCCTCC-TACCGAACTTCCACTCAGGA-3′; mismatched bases against the wild-type allele are underlined) and *pX330* with 5′-ACACAGAAAATCCAAGTTCA-3′ as a seed sequence. The R1170W (C to T) mutation was introduced into *Lrp4* by co-injecting an oligo donor (5′-TTGGCAACCTGGATGGGTC-TATGCGGAAAGTGTTGGTGTGGCAGAACCTTGACAGTCCCTG-GGCCATTGTATTATACCATGAAATGGGGTGAGAGCTGGCTTT-ATCACTCTGAGTGGAC-3′) and *pX330* with 5′-TGGTATAATA-CAATGGCCCG-3′ as a seed sequence. Both *Lrp4*$^{\Delta ICD}$ and *Lrp4*^{R1170W} mice were generated and maintained on the FVB/N strain (supplementary Materials and Methods).

X-Gal staining and *in situ* hybridization

To detect β-galactosidase activity from *lacZ* reporters, embryos were dissected and fixed in either 0.1% paraformaldehyde (PFA)/0.2% glutaraldehyde (E11.5-E13.5) or 4% PFA (E14.0 or older) for 30-60 min on ice. After washes in PBS, fixed samples were stained in X-Gal for 4-20 h at 4°C or at room temperature. Whole-mount *in situ* hybridization was performed with dissected jaws fixed in 4% PFA overnight according to standard protocols using DIG-labeled antisense riboprobes (Roche) against Lrp4 (Weatherbee et al., 2006) and Shh (Dassule and McMahon, 1998). For histological sections, stained samples were paraffin embedded after post-fixation in 4% PFA, sectioned at 8 µm and counterstained with Nuclear Fast Red.

Dual luciferase assay

HEK 293T cells were grown in DMEM (Dulbecco's Modified Eagle Medium with 4 mM glutamine, Gibco) supplemented with 10% FBS. Cells were plated on 24-well plates at ∼50% confluence, transfected with Lipofectamine 2000 (Thermo Fisher Scientific) the following day according to the manufacturer's protocol and harvested 24 h after transfection. Expression constructs were generated by inserting a full-length cDNA of each gene into the multicloning sites of pCS2+ (Turner and Weintraub, 1994). The amounts of individual DNA constructs used per well were 100 ng *TOPflash* (EMD Millipore), 5 ng *Renilla* luciferase, 100 ng *Wnt1* or human *WNT3A*, 100 ng *Lrp4* or *Lrp6* or chimeric receptors, and 200 ng *Wise* or *Sost*. The empty vector pCS2+ was added to the DNA mix to keep the total amount of DNA at ∼700 ng/well. Dual-luciferase reporter assays (Promega) were performed according to the manufacturer's protocol. Each experiment was performed in duplicate and representative results are from one of three independent experiments.

Acknowledgements

We thank Jenny Reynolds, Heidi Monnin and the Stowers Institute Histology Facility for technical assistance and members of the R.K. laboratory for valuable discussion.

Competing interests

The authors declare no competing or financial interests.

Author contributions

Conceptualization: Y.A., R.K.; Methodology: Y.A., R.K.; Validation: Y.A.; Formal analysis: Y.A., M.J.M., P.K.K., J.F.-A., R.K.; Investigation: Y.A., C.S., M.J.M., P.K.K., J.F.-A., S.D.W., R.K.; Resources: Y.A., C.S., S.D.W., R.K.; Data curation: Y.A., C.S.; Writing - original draft: Y.A., R.K.; Writing - review & editing: Y.A., S.D.W., R.K.; Visualization: Y.A., R.K.; Supervision: Y.A., R.K.; Project administration: C.S., R.K.; Funding acquisition: R.K.

Funding

Y.A., C.S., M.J.M., P.K.K., J.F.-A. and R.K. were supported by funds from Stowers Institute for Medical Research, and S.D.W. was supported by a grant from the National Institutes of Health (R01AR059687). Deposited in PMC for release after 12 months.

Data availability

Original data underlying this manuscript can be accessed from the Stowers Original Data Repository at http://www.stowers.org/research/publications/libpb-1185.

Supplementary information

Supplementary information available online at
http://dev.biologists.org/lookup/doi/10.1242/dev.150680.supplemental

References

Ahn, Y. (2015). Signaling in tooth, hair, and mammary placodes. *Curr. Top. Dev. Biol.* **111**, 421-459.

Ahn, Y., Sanderson, B. W., Klein, O. D. and Krumlauf, R. (2010). Inhibition of Wnt signaling by Wise (Sostdc1) and negative feedback from Shh controls tooth number and patterning. *Development* **137**, 3221-3231.

Ahn, Y., Sims, C., Logue, J. M., Weatherbee, S. D. and Krumlauf, R. (2013). Lrp4 and Wise interplay controls the formation and patterning of mammary and other skin appendage placodes by modulating Wnt signaling. *Development* **140**, 583-593.

Balic, A. and Thesleff, I. (2015). Tissue interactions regulating tooth development and renewal. *Curr. Top. Dev. Biol.* **115**, 157-186.

Biggs, L. C. and Mikkola, M. L. (2014). Early inductive events in ectodermal appendage morphogenesis. *Semin. Cell Dev. Biol.* **25-26**, 11-21.
Chang, M.-K., Kramer, I., Huber, T., Kinzel, B., Guth-Gundel, S., Leupin, O. and Kneissel, M. (2014a). Disruption of Lrp4 function by genetic deletion or pharmacological blockade increases bone mass and serum sclerostin levels. *Proc. Natl. Acad. Sci. USA* **111**, E5187-E5195.
Chang, M.-K., Kramer, I., Keller, H., Gooi, J. H., Collett, C., Jenkins, D., Ettenberg, S. A., Cong, F., Halleux, C. and Kneissel, M. (2014b). Reversing LRP5-dependent osteoporosis and SOST deficiency-induced sclerosing bone disorders by altering WNT signaling activity. *J. Bone Miner. Res.* **29**, 29-42.
Choi, H. Y., Dieckmann, M., Herz, J. and Niemeier, A. (2009). Lrp4, a novel receptor for Dickkopf 1 and sclerostin, is expressed by osteoblasts and regulates bone growth and turnover in vivo. *PLoS ONE* **4**, e7930.
Choi, H. Y., Liu, Y., Tennert, C., Sugiura, Y., Karakatsani, A., Kroger, S., Johnson, E. B., Hammer, R. E., Lin, W. and Herz, J. (2013). APP interacts with LRP4 and agrin to coordinate the development of the neuromuscular junction in mice. *Elife* **2**, e00220.
Clevers, H. and Nusse, R. (2012). Wnt/beta-catenin signaling and disease. *Cell* **149**, 1192-1205.
Collette, N. M., Genetos, D. C., Economides, A. N., Xie, L., Shahnazari, M., Yao, W., Lane, N. E., Harland, R. M. and Loots, G. G. (2012). Targeted deletion of Sost distal enhancer increases bone formation and bone mass. *Proc. Natl. Acad. Sci. USA* **109**, 14092-14097.
Collette, N. M., Yee, C. S., Murugesh, D., Sebastian, A., Taher, L., Gale, N. W., Economides, A. N., Harland, R. M. and Loots, G. G. (2013). Sost and its paralog Sostdc1 coordinate digit number in a Gli3-dependent manner. *Dev. Biol.* **383**, 90-105.
Cong, L., Ran, F. A., Cox, D., Lin, S., Barretto, R., Habib, N., Hsu, P. D., Wu, X., Jiang, W., Marraffini, L. A. et al. (2013). Multiplex genome engineering using CRISPR/Cas systems. *Science* **339**, 819-823.
Cruciat, C.-M. and Niehrs, C. (2013). Secreted and transmembrane wnt inhibitors and activators. *Cold Spring Harb. Perspect. Biol.* **5**, a015081.
DasGupta, R. and Fuchs, E. (1999). Multiple roles for activated LEF/TCF transcription complexes during hair follicle development and differentiation. *Development* **126**, 4557-4568.
Dassule, H. R. and McMahon, A. P. (1998). Analysis of epithelial-mesenchymal interactions in the initial morphogenesis of the mammalian tooth. *Dev. Biol.* **202**, 215–227.
Dietrich, M. F., van der Weyden, L., Prosser, H. M., Bradley, A., Herz, J. and Adams, D. J. (2010). Ectodomains of the LDL receptor-related proteins LRP1b and LRP4 have anchorage independent functions in vivo. *PLoS ONE* **5**, e9960.
Ellies, D. L. and Krumlauf, R. (2006). Bone formation: the nuclear matrix reloaded. *Cell* **125**, 840-842.
Gomez, A. M. and Burden, S. J. (2011). The extracellular region of Lrp4 is sufficient to mediate neuromuscular synapse formation. *Dev. Dyn.* **240**, 2626-2633.
Gossen, M. and Bujard, H. (1992). Tight control of gene expression in mammalian cells by tetracycline-responsive promoters. *Proc. Natl. Acad. Sci. USA* **89**, 5547-5551.
Herz, J. and Bock, H. H. (2002). Lipoprotein receptors in the nervous system. *Annu. Rev. Biochem.* **71**, 405-434.
Itasaki, N., Jones, C. M., Mercurio, S., Rowe, A., Domingos, P. M., Smith, J. C. and Krumlauf, R. (2003). Wise, a context-dependent activator and inhibitor of Wnt signalling. *Development* **130**, 4295-4305.
Johnson, E. B., Hammer, R. E. and Herz, J. (2005). Abnormal development of the apical ectodermal ridge and polysyndactyly in Megf7-deficient mice. *Hum. Mol. Genet.* **14**, 3523-3538.
Karner, C. M., Dietrich, M. F., Johnson, E. B., Kappesser, N., Tennert, C., Percin, F., Wollnik, B., Carroll, T. J. and Herz, J. (2010). Lrp4 regulates initiation of ureteric budding and is crucial for kidney formation–a mouse model for Cenani-Lenz syndrome. *PLoS ONE* **5**, e10418.
Kato, M., Patel, M. S., Levasseur, R., Lobov, I., Chang, B. H.-J., Glass, D. A., II, Hartmann, C., Li, L., Hwang, T.-H., Brayton, C. F. et al. (2002). Cbfa1-independent decrease in osteoblast proliferation, osteopenia, and persistent embryonic eye vascularization in mice deficient in Lrp5, a Wnt coreceptor. *J. Cell Biol.* **157**, 303-314.
Kavanagh, K. D., Evans, A. R. and Jernvall, J. (2007). Predicting evolutionary patterns of mammalian teeth from development. *Nature* **449**, 427-432.
Laurikkala, J., Kassai, Y., Pakkasjarvi, L., Thesleff, I. and Itoh, N. (2003). Identification of a secreted BMP antagonist, ectodin, integrating BMP, FGF, and SHH signals from the tooth enamel knot. *Dev. Biol.* **264**, 91-105.
Lee, E.-C., Yu, D., Martinez de Velasco, J., Tessarollo, L., Swing, D. A., Court, D. L., Jenkins, N. A. and Copeland, N. G. (2001). A highly efficient Escherichia coli-based chromosome engineering system adapted for recombinogenic targeting and subcloning of BAC DNA. *Genomics* **73**, 56-65.
Leupin, O., Piters, E., Halleux, C., Hu, S., Kramer, I., Morvan, F., Bouwmeester, T., Schirle, M., Bueno-Lozano, M., Ramos Fuentes, F. J. et al. (2011). Bone overgrowth-associated mutations in the LRP4 gene impair sclerostin facilitator function. *J. Biol. Chem.* **286**, 19489-19500.
Li, X., Zhang, Y., Kang, H., Liu, W., Liu, P., Zhang, J., Harris, S. E. and Wu, D. (2005). Sclerostin binds to LRP5/6 and antagonizes canonical Wnt signaling. *J. Biol. Chem.* **280**, 19883-19887.
Li, X., Ominsky, M. S., Niu, Q.-T., Sun, N., Daugherty, B., D'Agostin, D., Kurahara, C., Gao, Y., Cao, J., Gong, J. et al. (2008). Targeted deletion of the sclerostin gene in mice results in increased bone formation and bone strength. *J. Bone Miner. Res.* **23**, 860-869.
Li, Y., Pawlik, B., Elcioglu, N., Aglan, M., Kayserili, H., Yigit, G., Percin, F., Goodman, F., Nürnberg, G., Cenani, A. et al. (2010). LRP4 mutations alter Wnt/β-catenin signaling and cause limb and kidney malformations in Cenani-Lenz syndrome. *Am. J. Hum. Genet.* **86**, 696-706.
MacDonald, B. T. and He, X. (2012). Frizzled and LRP5/6 receptors for Wnt/beta-catenin signaling. *Cold Spring Harb. Perspect. Biol.* **4**, a007880.
MacDonald, B. T., Tamai, K. and He, X. (2009). Wnt/beta-catenin signaling: components, mechanisms, and diseases. *Dev. Cell* **17**, 9-26.
Mashiko, D., Fujihara, Y., Satouh, Y., Miyata, H., Isotani, A. and Ikawa, M. (2013). Generation of mutant mice by pronuclear injection of circular plasmid expressing Cas9 and single guided RNA. *Sci. Rep.* **3**, 3355.
Narhi, K., Tummers, M., Ahtiainen, L., Itoh, N., Thesleff, I. and Mikkola, M. L. (2012). Sostdc1 defines the size and number of skin appendage placodes. *Dev. Biol.* **364**, 149-161.
Ohazama, A., Johnson, E. B., Ota, M. S., Choi, H. J., Porntaveetus, T., Oommen, S., Itoh, N., Eto, K., Gritli-Linde, A., Herz, J. et al. (2008). Lrp4 modulates extracellular integration of cell signaling pathways in development. *PLoS ONE* **3**, e4092.
Peterkova, R., Lesot, H. and Peterka, M. (2006). Phylogenetic memory of developing mammalian dentition. *J. Exp. Zoolog. B Mol. Dev. Evol.* **306B**, 234-250.
Pinson, K. I., Brennan, J., Monkley, S., Avery, B. J. and Skarnes, W. C. (2000). An LDL-receptor-related protein mediates Wnt signalling in mice. *Nature* **407**, 535-538.
Pohlkamp, T., Durakoglugil, M., Lane-Donovan, C., Xian, X., Johnson, E. B., Hammer, R. E. and Herz, J. (2015). Lrp4 domains differentially regulate limb/brain development and synaptic plasticity. *PLoS ONE* **10**, e0116701.
Semenov, M., Tamai, K. and He, X. (2005). SOST is a ligand for LRP5/LRP6 and a Wnt signaling inhibitor. *J. Biol. Chem.* **280**, 26770-26775.
Shen, C., Xiong, W.-C. and Mei, L. (2015). LRP4 in neuromuscular junction and bone development and diseases. *Bone* **80**, 101-108.
Simon-Chazottes, D., Tutois, S., Kuehn, M., Evans, M., Bourgade, F., Cook, S., Davisson, M. T. and Guenet, J.-L. (2006). Mutations in the gene encoding the low-density lipoprotein receptor LRP4 cause abnormal limb development in the mouse. *Genomics* **87**, 673-677.
Turner, D. L. and Weintraub, H. (1994). Expression of achaete-scute homolog 3 in Xenopus embryos converts ectodermal cells to a neural fate. *Genes Dev.* **8**, 1434-1447.
Wang, H., Yang, H., Shivalila, C. S., Dawlaty, M. M., Cheng, A. W., Zhang, F. and Jaenisch, R. (2013). One-step generation of mice carrying mutations in multiple genes by CRISPR/Cas-mediated genome engineering. *Cell* **153**, 910-918.
Weatherbee, S. D., Anderson, K. V. and Niswander, L. A. (2006). LDL-receptor-related protein 4 is crucial for formation of the neuromuscular junction. *Development* **133**, 4993-5000.
Willnow, T. E., Christ, A. and Hammes, A. (2012). Endocytic receptor-mediated control of morphogen signaling. *Development* **139**, 4311-4319.
Xiong, L., Jung, J.-U., Wu, H., Xia, W.-F., Pan, J.-X., Shen, C., Mei, L. and Xiong, W.-C. (2015). Lrp4 in osteoblasts suppresses bone formation and promotes osteoclastogenesis and bone resorption. *Proc. Natl. Acad. Sci. USA* **112**, 3487-3492.

SUPPLEMENTARY MATERIALS AND METHODS

Generation of *Lrp4*^{LacZ}, *Lrp4*$^{\Delta ICD}$, *Lrp4*^{R1170W} mice using the CRISPR/Cas9 technology

For an in-frame insertion of *LacZ* into the first exon of Lrp4, a donor plasmid was generated by capturing the *LacZ-SV40polyA* cassette and flanking regions from the *Lrp4-LacZ* BAC clone (Ahn et al., 2013). The resulting plasmid contains left and right homology arms from the *Lrp4* locus (2.3 kb and 1.0 kb, respectively). Germline transmission of the targeted allele was achieved by crossing a founder with wild-type C57BL/10JxCBA-F1 mice.

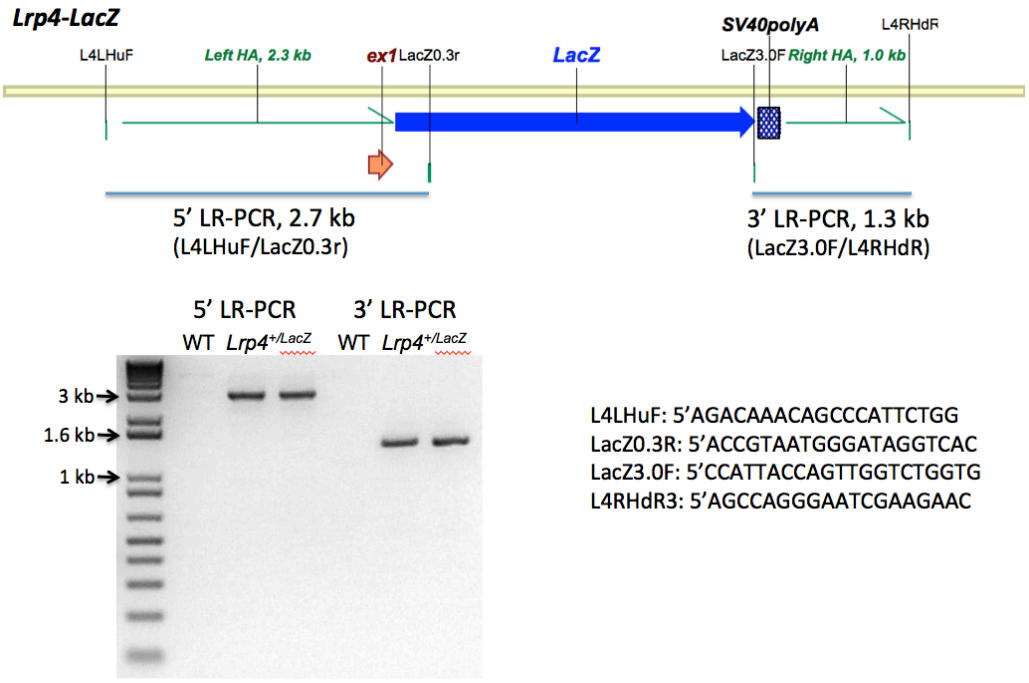

After successful germline transmission, correct targeting was confirmed in mice heterozygous for the *LacZ* knock-in allele (*Lrp4*$^{+/LacZ}$) by long-range PCR with combinations of primers, one of which is external to the homology arms (see the figure above). The strain was maintained as heterozygotes since mice homozygous for the allele are not viable.

Lrp4$^{\Delta ICD}$ and *Lrp4*^{R1170W} mice were generated by co-injecting a pX330 plasmid and an oligo donor with the desired mutation into FVB/N embryos. For each model, two founder mice were bred to wild-type FVB/N mice for germline transmission. Correct targeting was confirmed by PCR amplification and sequencing of the targeted regions from heterozygous mice (see the figure below). Primers used for the PCR are,
Lrp4$^{\Delta ICD}$: 5'-TCCATCTGTCCCCCAGCATC and 5'-CTTTCTCACCCACTCAGGCA
Lrp4^{R1170W}: 5'-GCTCACAGCATGAGGACATC and 5'-TGCTCCTATGCTTCATGGTC

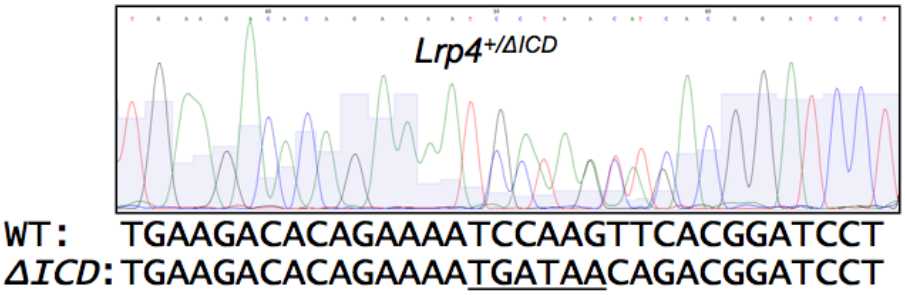

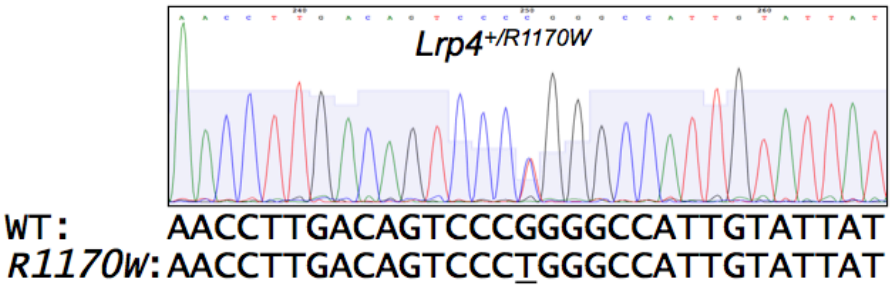

After successful germline transmission, heterozygous mice from individual founders were crossed to generate homozygous mice. Homozygous *Lrp4*$^{\Delta ICD}$ and *Lrp4*^{R1170W} mice are viable and two independent lines with the same mutation display tooth phenotypes indistinguishable from each other.

For generation of the *Lrp4*^{LacZ}, *Lrp4*$^{\Delta ICD}$, *Lrp4*^{R1170W} mice with CRISPR/Cas9 technology, seed sequences were carefully selected to minimize potential risk of off-target effect. Specifically, the selected seed sequences do not have any potential off-target with off-target score over 2.0 (www.benchling.com) across the whole mouse genome.

Ahn, Y., Sims, C., Logue, J.M., Weatherbee, S.D., Krumlauf, R., 2013. Lrp4 and Wise interplay controls the formation and patterning of mammary and other skin appendage placodes by modulating Wnt signaling. Development 140, 583-593.

Supplementary Table S1. Summary of mouse strains used in the study

Gene	Allele	Modification/Purpose	Gene function	Reference
Lrp4	*mitt*	Premature stop codon in exon 10	null	Weatherbee et al., 2006
Lrp4	*mte*	D1436G missense mutation	null	Weatherbee et al., 2006
Lrp4	*LacZ*	*LacZ* insertion into exon 1	null	this study
Lrp4	*ECD*	Insertion of a stop codon before the transmemebrane domain	hypomorphic	Johnson et al., 2005
Lrp4	*mdig*	A point mutations causing skipping of exon 15	hypomorphic	Simon-Chazottes et al., 2006
Lrp4	*R1170W*	R1170W misssense mutation	hypomorphic	this study
Lrp4	*ΔICD*	Insertion of a stop codon after the transmemebrane domain	hypomorphic	this study
Lrp4	*tetO-Lrp4*	Random integration/tTA-dependent over-expression	gain-of-function	this study
Lrp4-Lrp6	*tetO-Lrp4ECDLrp6ICD*	Random integration/tTA-dependent over-expression	gain-of-function	this study
Lrp4	*Lrp4BAC-tTA*	Random integration/tTA expression from an *Lrp4* BAC clone	tTA driver	this study
Lrp5	*null*	Insertion of *IRES-LacZ-Neo* at amino acid 373	null	Kato et al., 2002
Lrp6	*null*	Insertion of *LacZ* at amino acid 321	null	Pinson et al., 2000
Lrp6	*tetO-Lrp6*	Random integration/tTA-dependent over-expression	gain-of-function	this study
Wise	*null*	*LacZ* insertion into exon 1	null	Ahn et al., 2010
Wise	*tetO-Wise*	Random integration/tTA-dependent over-expression	gain-of-function	Ahn et al., 2013
KRT14	*K14-tTA*	Random integration/tTA expression driven by a human *KRT14* promoter	tTA driver	Ahn et al., 2013

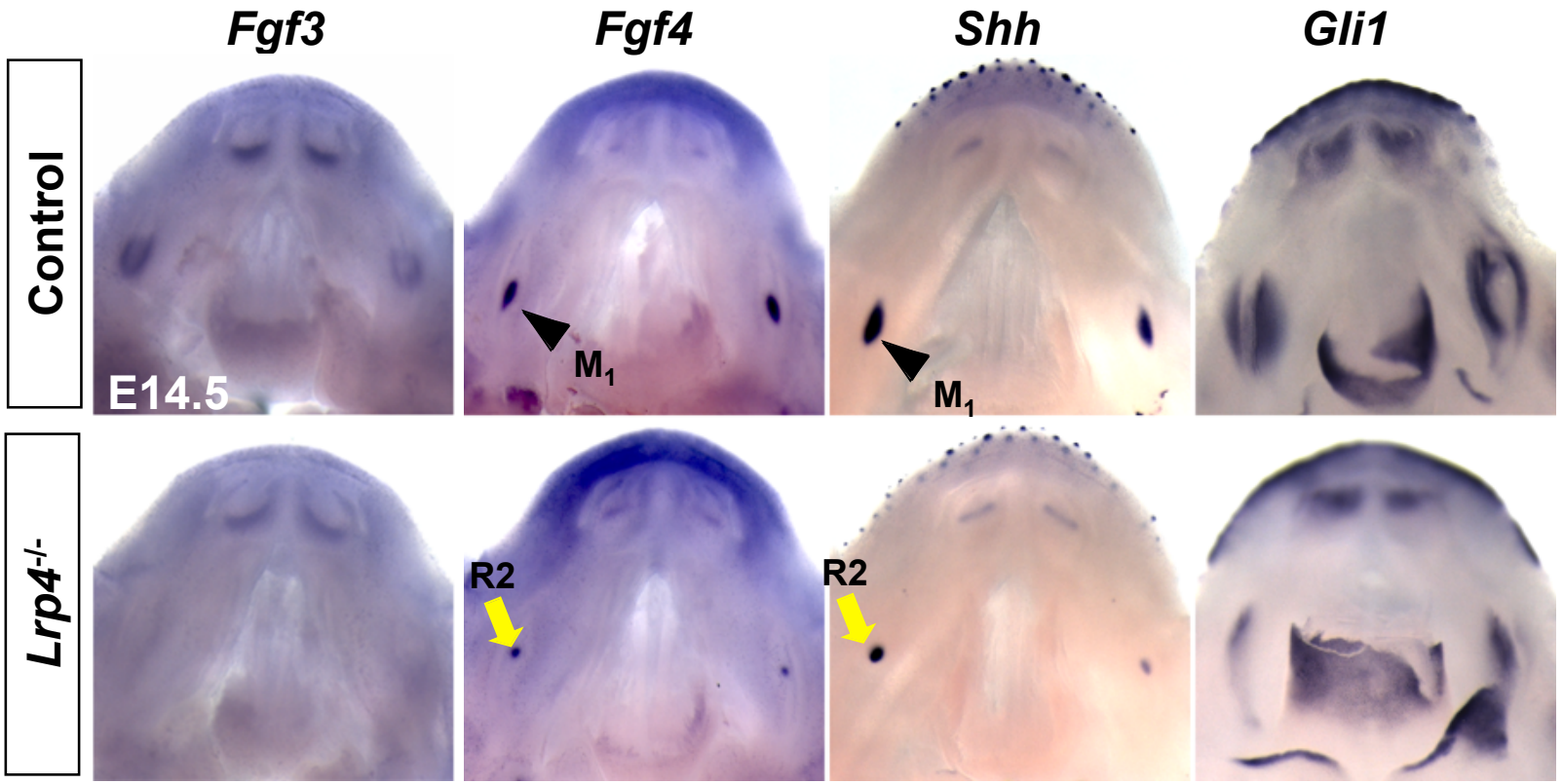

Suppl. Fig. S1. Abnormal embryonic tooth development in *Lrp4*-null mice.

Differential gene expression at E14.5 in the tooth germ of *Lrp4*-null mice shown by *in situ* hybridization with mandibles. Control mice are wild-type or heterozygous for either $Lrp4^{mitt}$ or $Lrp4^{mte}$ allele and $Lrp4^{-/-}$ mice are homozygous for either $Lrp4^{mitt}$ or $Lrp4^{mte}$ allele.

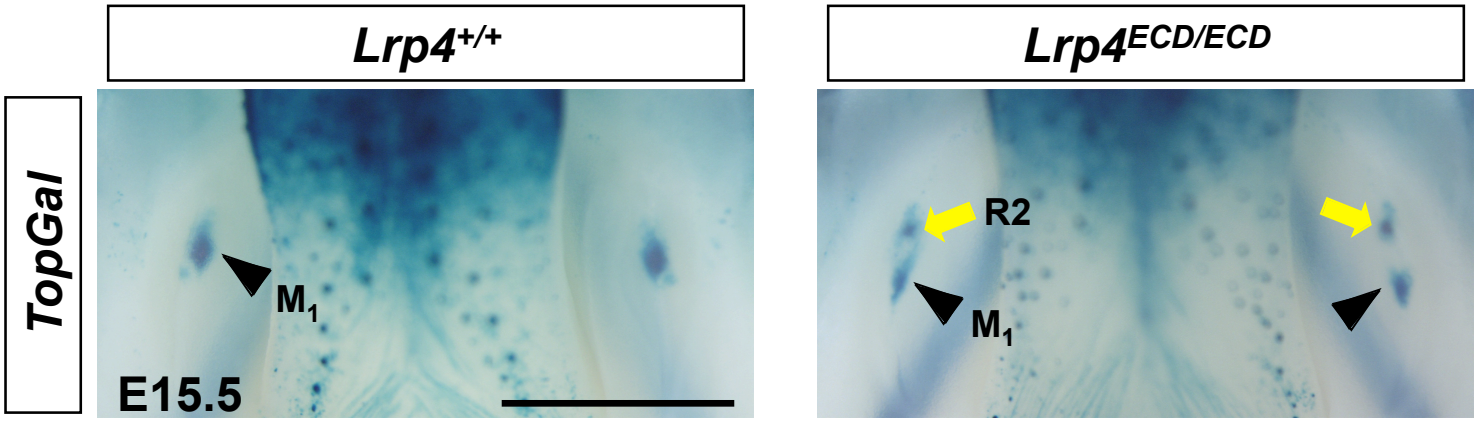

Suppl. Fig. S2. Abnormal *TopGal* expression pattern in teeth of *Lrp4*$^{ECD/ECD}$ mice.

TopGal staining indicates that R2 gives rise to a supernumerary tooth in *Lrp4*$^{ECD/ECD}$ mice. Similar to *Lrp4*-null mice, these mice display variable distance between R2 and M_1. Scale bar 1 mm.

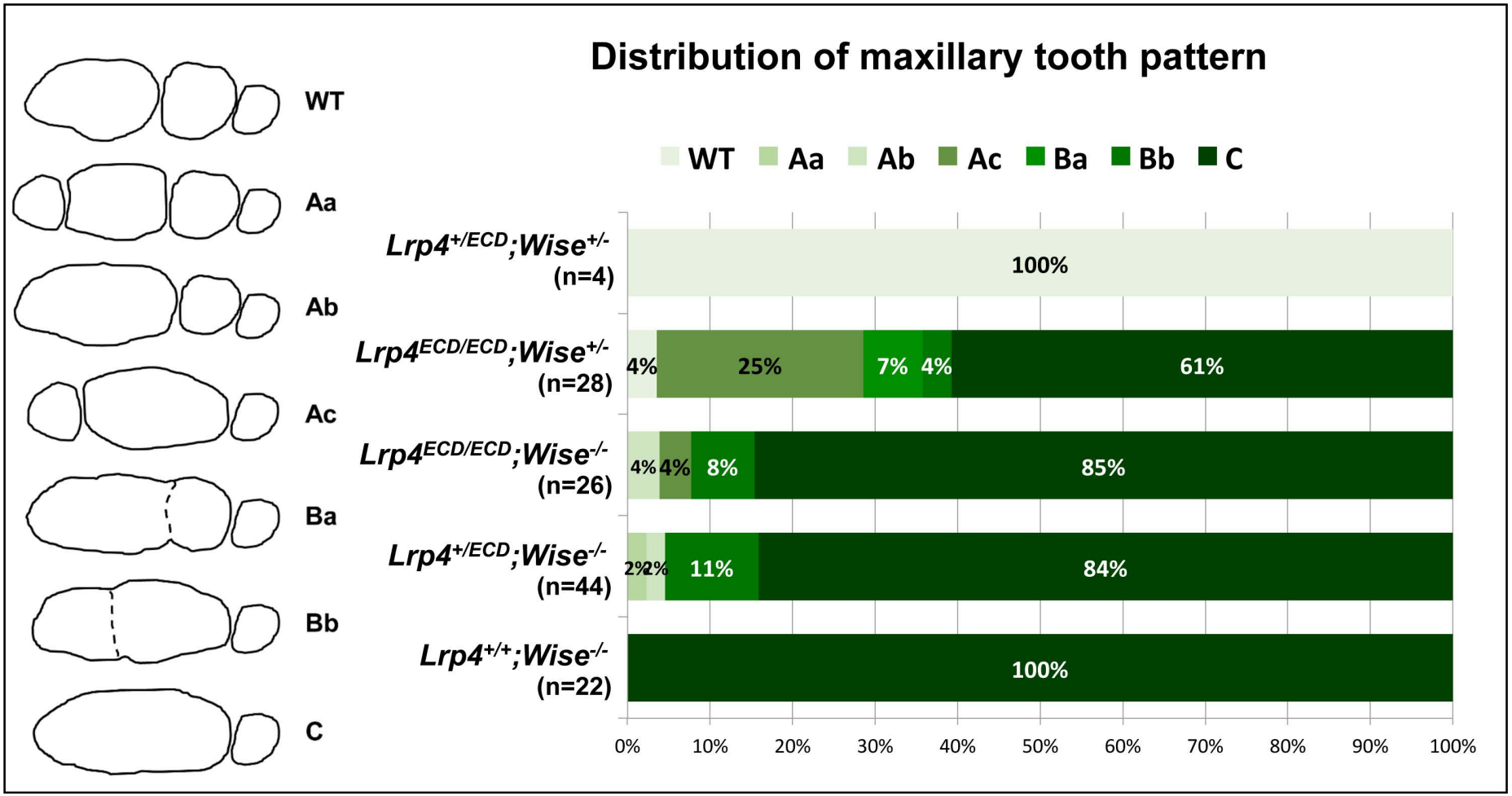

Suppl. Fig. S3. *Lrp4* deficiency ameliorates *Wise*-null tooth defects in the maxilla.

Maxillary tooth patterns are categorized based on the number, size and fusion of cheek teeth (left). Distribution of different tooth patterns among littermates of the $Lrp4^{ECD}$ and *Wise*-null combinatorial mutants (right).

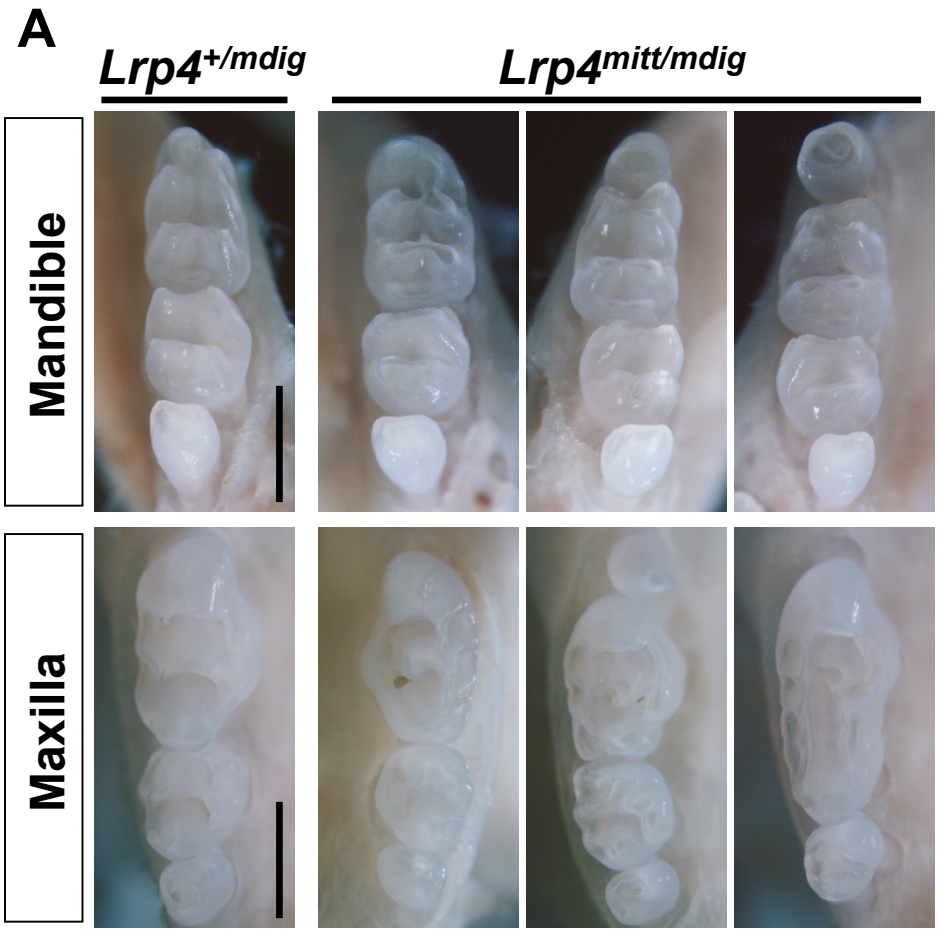

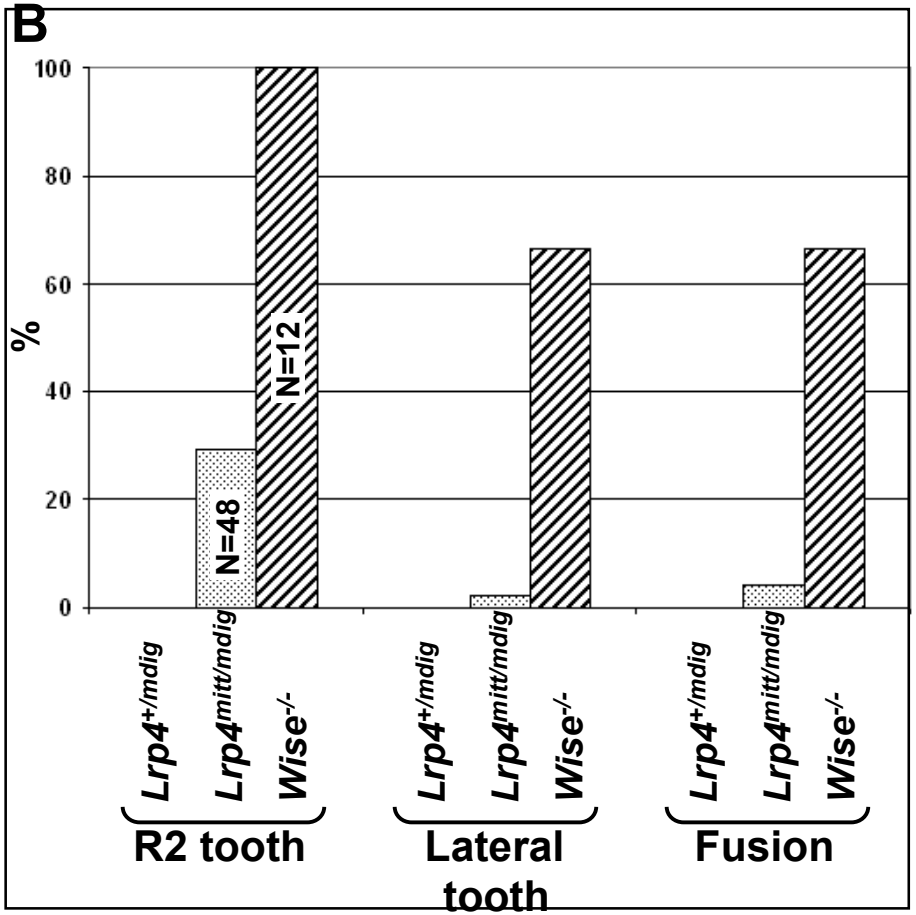

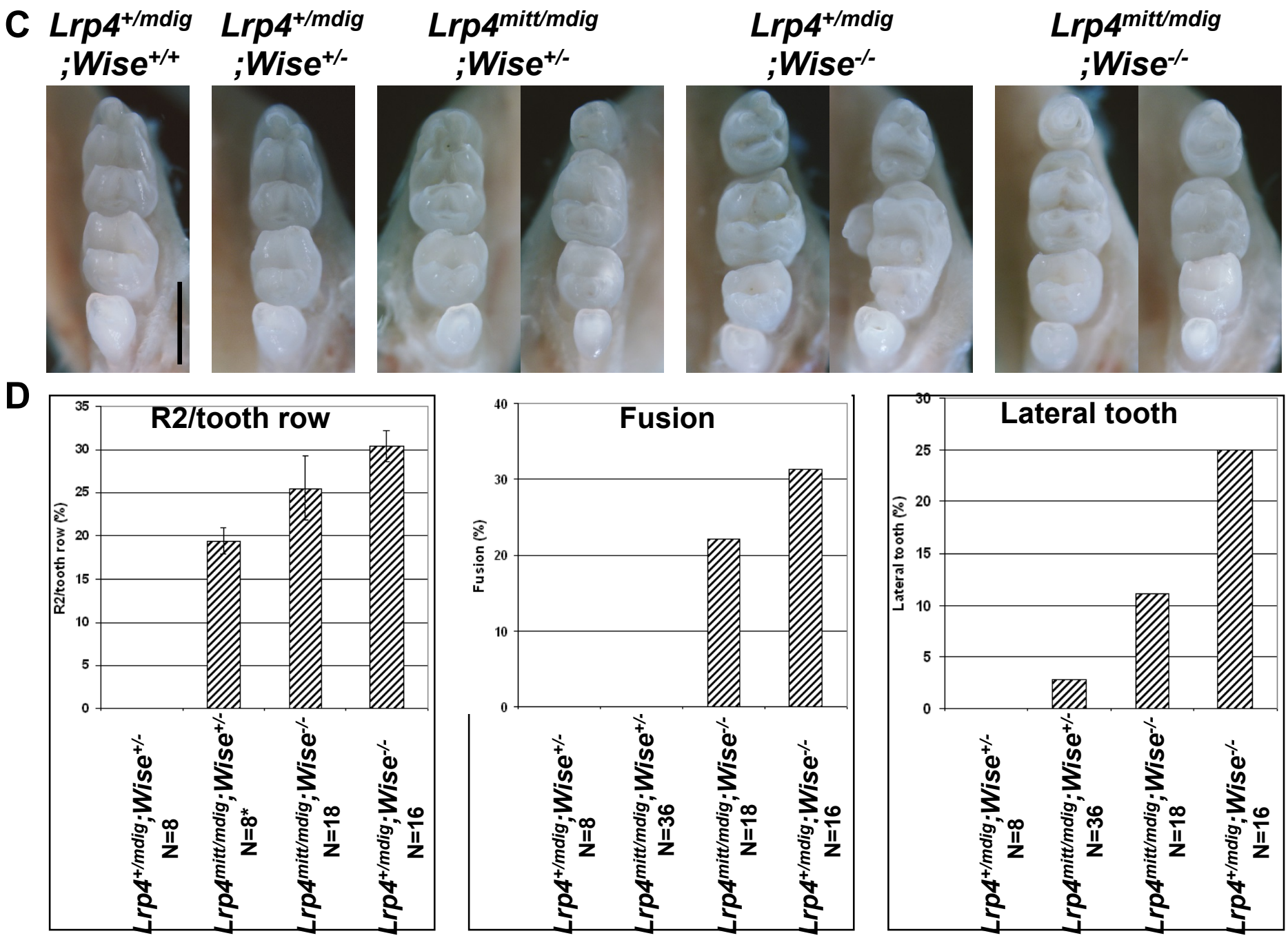

Suppl. Fig. S4. *Lrp4* deficiency ameliorates *Wise*-null tooth defects.

(A) Representative tooth patterns of *Lrp4*$^{mitt/mdig}$ mice.
(B) *Lrp4*$^{mitt/mdig}$ mice display variable, but generally milder tooth defects in the mandible compared to *Wise*-null mice.
(C) Representative tooth patterns of *Lrp4* and *Wise* combinatorial mutants.
(D) *Lrp4* deficiency ameliorates tooth defects of *Wise*-null mice in a dose dependent manner in the mandible. Relative size of R2 (left) and frequency of molar fusion (middle) and lateral supernumerary teeth (right) per jaw quadrant were scored among littermates. *: only 8 quadrants with a R2 tooth were scored and the others (28) had the normal three-molar pattern.
Scale bar 1 mm.

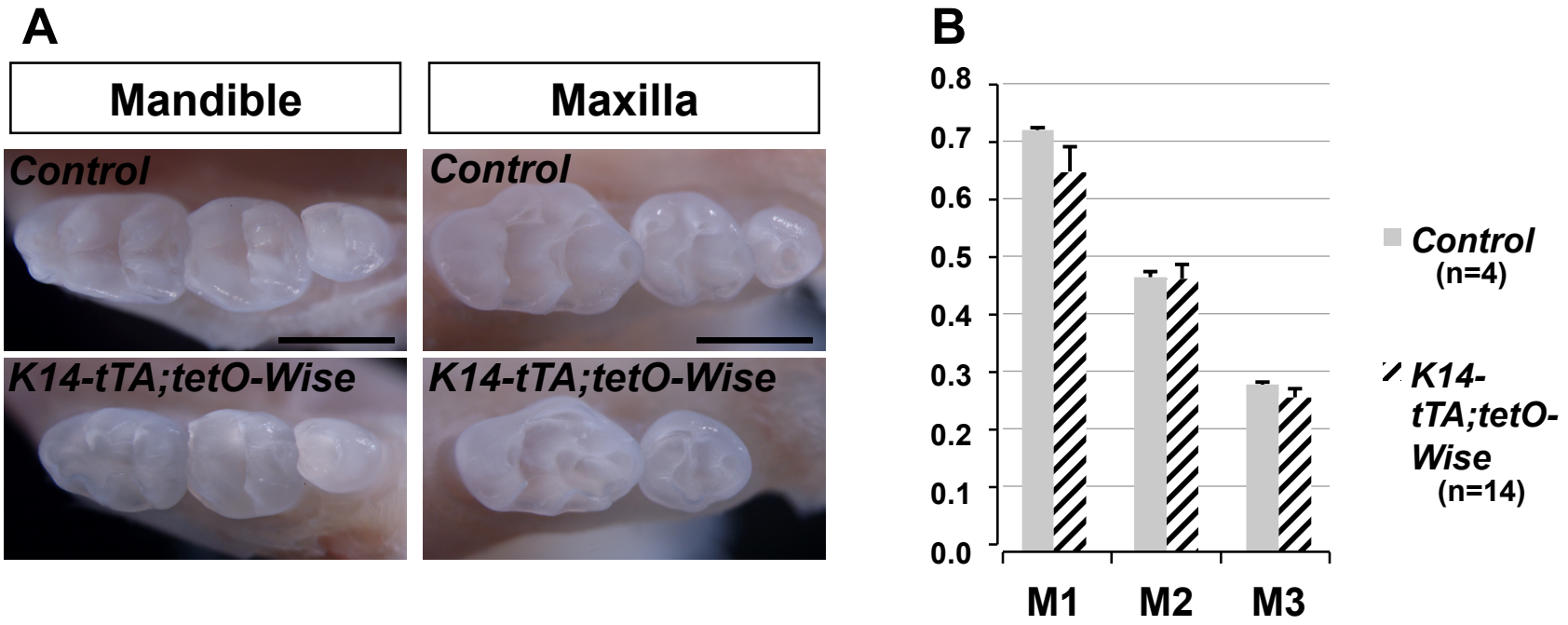

Suppl. Fig. S5. *Wise* over-expression disrupts tooth development.

(A) Molars are generally smaller and in the maxilla M_3 is often missing (28.6%, 4/14) in *K14-tTA;tetO-Wise* mice. Scale bar 1 mm.
(B) Mandibular M_1 and M_3 are significantly smaller in *K14-tTA;tetO-Wise* mice (M_1: p=0.0036; M_3: p=0.045) while M_2 are similar in size. Error bar: standard deviation

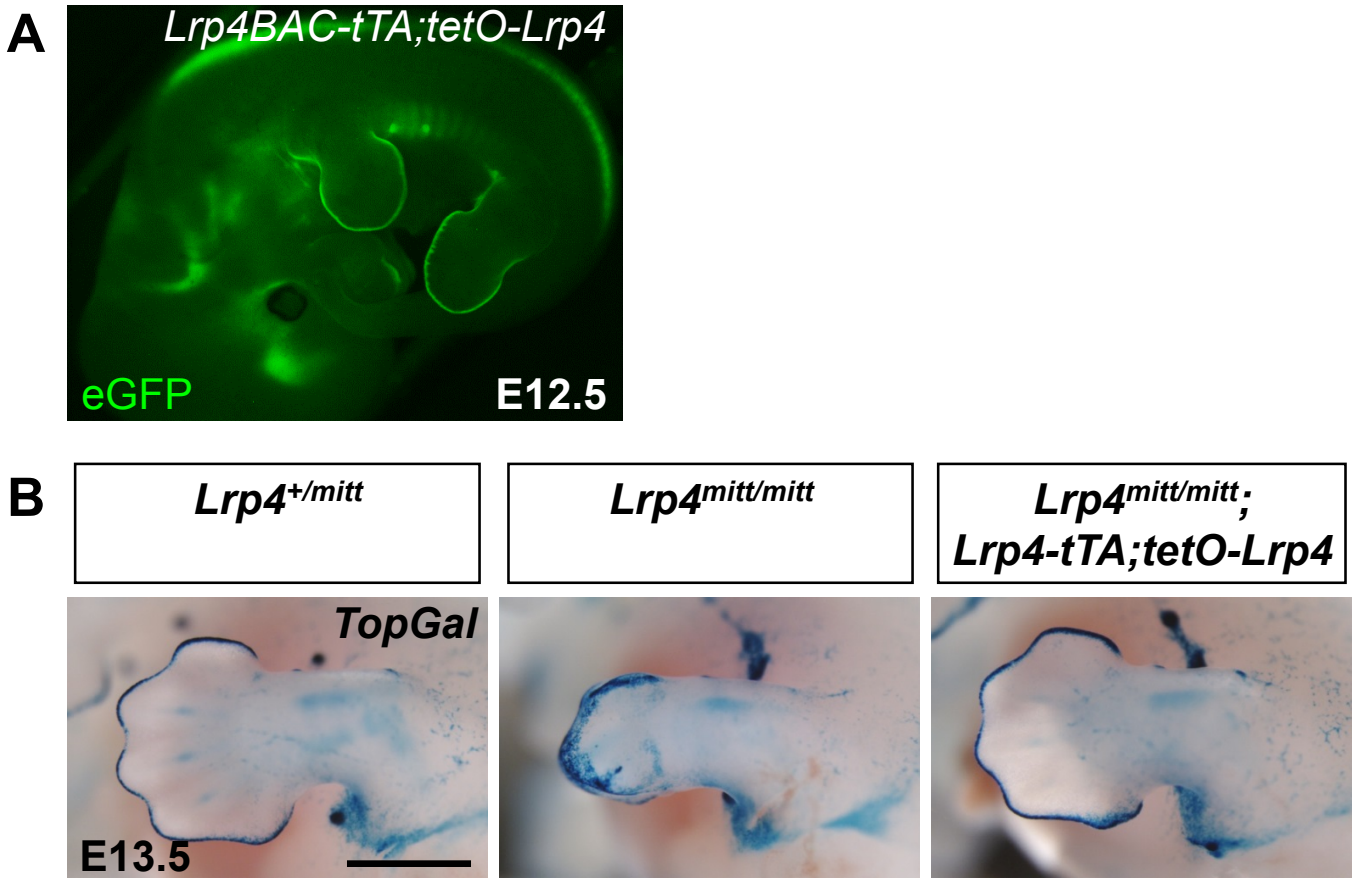

Suppl. Fig. S6. Transgenic *Lrp4* expression rescues *Lrp4*-null limb defect.

(A) eGFP expression driven by *Lrp4* BAC-tTA transgene which recapitulates the endogenous *Lrp4* expression pattern in the limb buds.
(B) *TopGal* expression indicates abnormal patterning of the distal limb in $Lrp4^{mitt/mitt}$ mice is rescued by transgenic *Lrp4* expression.
Scale bar 1 mm.

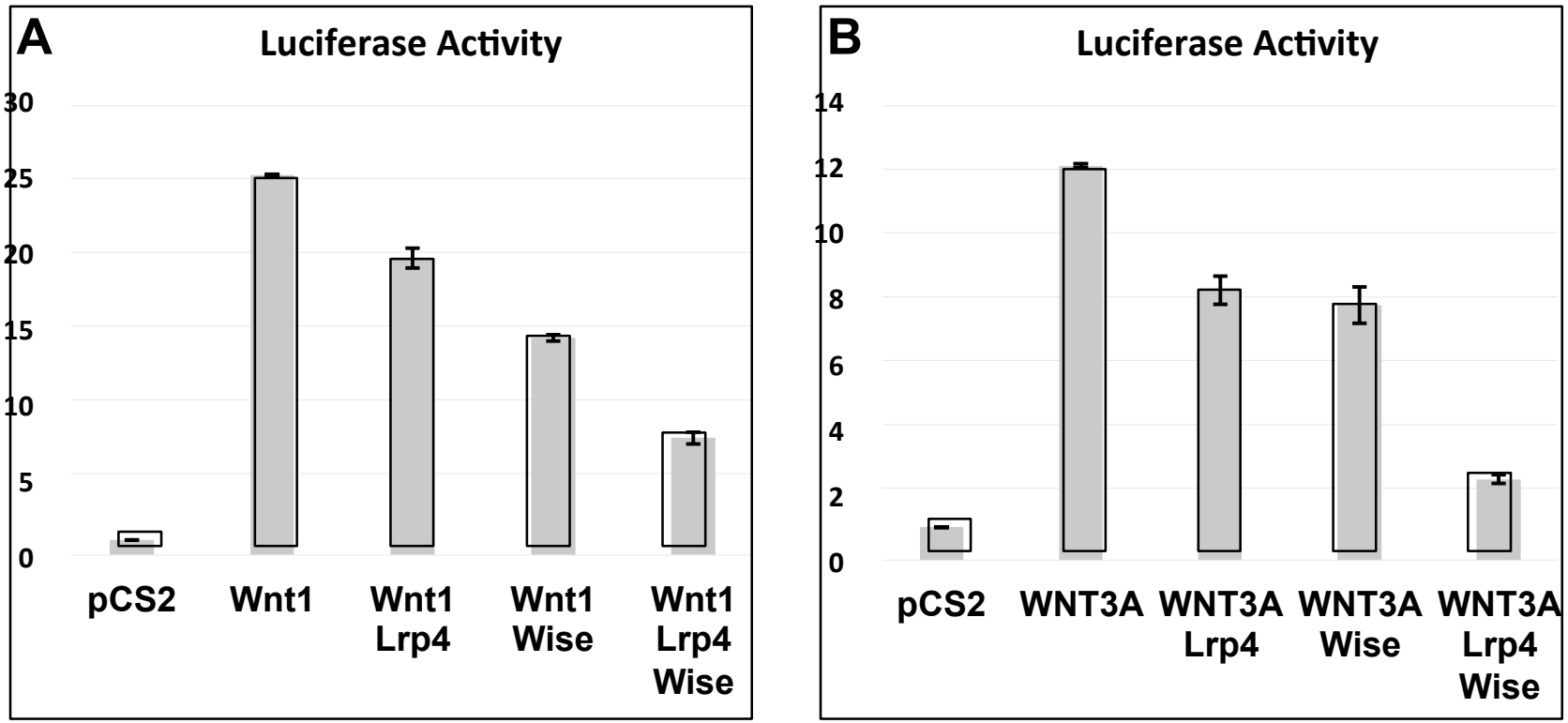

Suppl. Fig. S7. *Lrp4* and *Wise* cooperatively inhibit Wnt/β-catenin signaling *in vitro*.

(A) Relative luciferase activity from TOPflash reporter activated by Wnt1. HEK 293T cells were transfected with an empty vector (pCS2) or constructs driving expression of Lrp4 or Wise.
(B) Relative luciferase activity from TOPflash reporter activated by WNT3A.

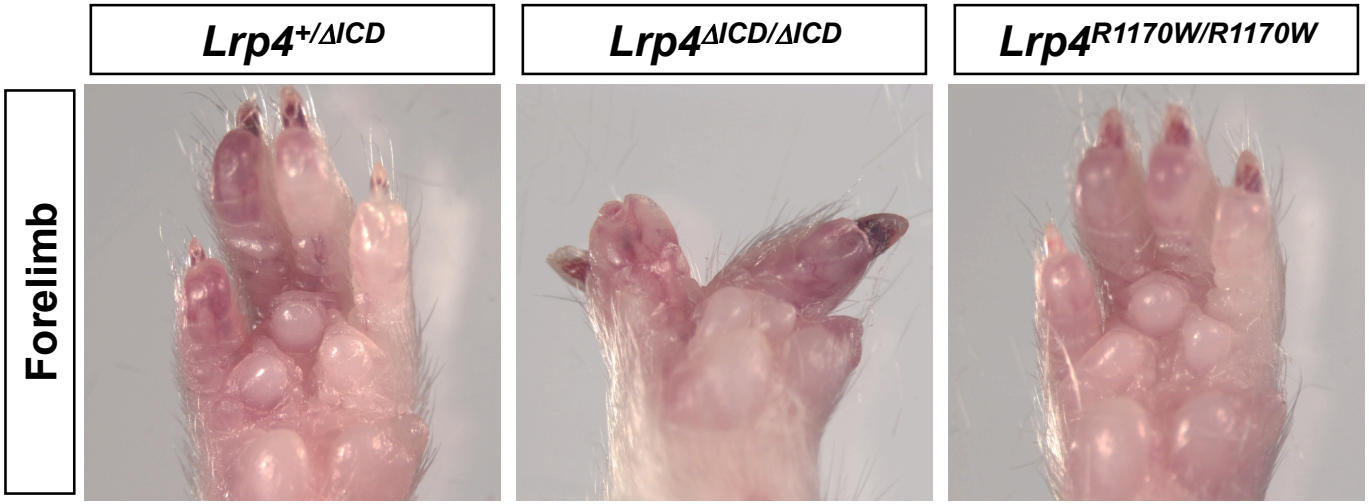

Suppl. Fig. S8. Limb phenotypes of *Lrp4*$^{\Delta ICD/\Delta ICD}$ and *Lrp4*$^{R1170W/R1170W}$ mice.

While the intracellular domain is essential for distal limb patterning (middle), the R1170W mutation does not have significant effect on limb patterning (right).